Supplementary Information

Hunger states modulate aggression via opposing dopamine pathways

Junlong Wang,[1,2,3,4,6] Qiantao Lv,[1,2,3,4,6] Yunming Gao,[2,3,4] Yaokai Yang,[2,3,4] Jing Ning,[2,3,4] Dandan Chen,[2,3,4] Wenjing Wang,[2,3,4,5] Xingjiang Zhang,[2,3,4] Zhou Li,[1,2,3,4] Yefeng Shao,[2,3,4,5] Qiong Liu,[2,3,4,5] Qiancheng Liang, [1,2,3,4] & Yi Sun[1,2,3,4,5]*

[1]College of Life Sciences, Zhejiang University, Hangzhou, China.

[2]Research Center for Industries of the Future and Key Laboratory of Growth Regulation and Translational Research of Zhejiang Province, School of Life Sciences, Westlake University, Hangzhou, China.

[3]Westlake Laboratory of Life Sciences and Biomedicine, Hangzhou, China.

[4]Institute of Basic Medical Sciences, Westlake Institute for Advanced Study, Hangzhou, China.

[5]Fudan University, Shanghai, China.

[6]These authors contributed equally: Junlong Wang, Qiantao Lv.

*e-mail: sunyi@westlake.edu.cn (Y.S.)

Supplementary Fig. 1-10

Supplementary Table 1-2

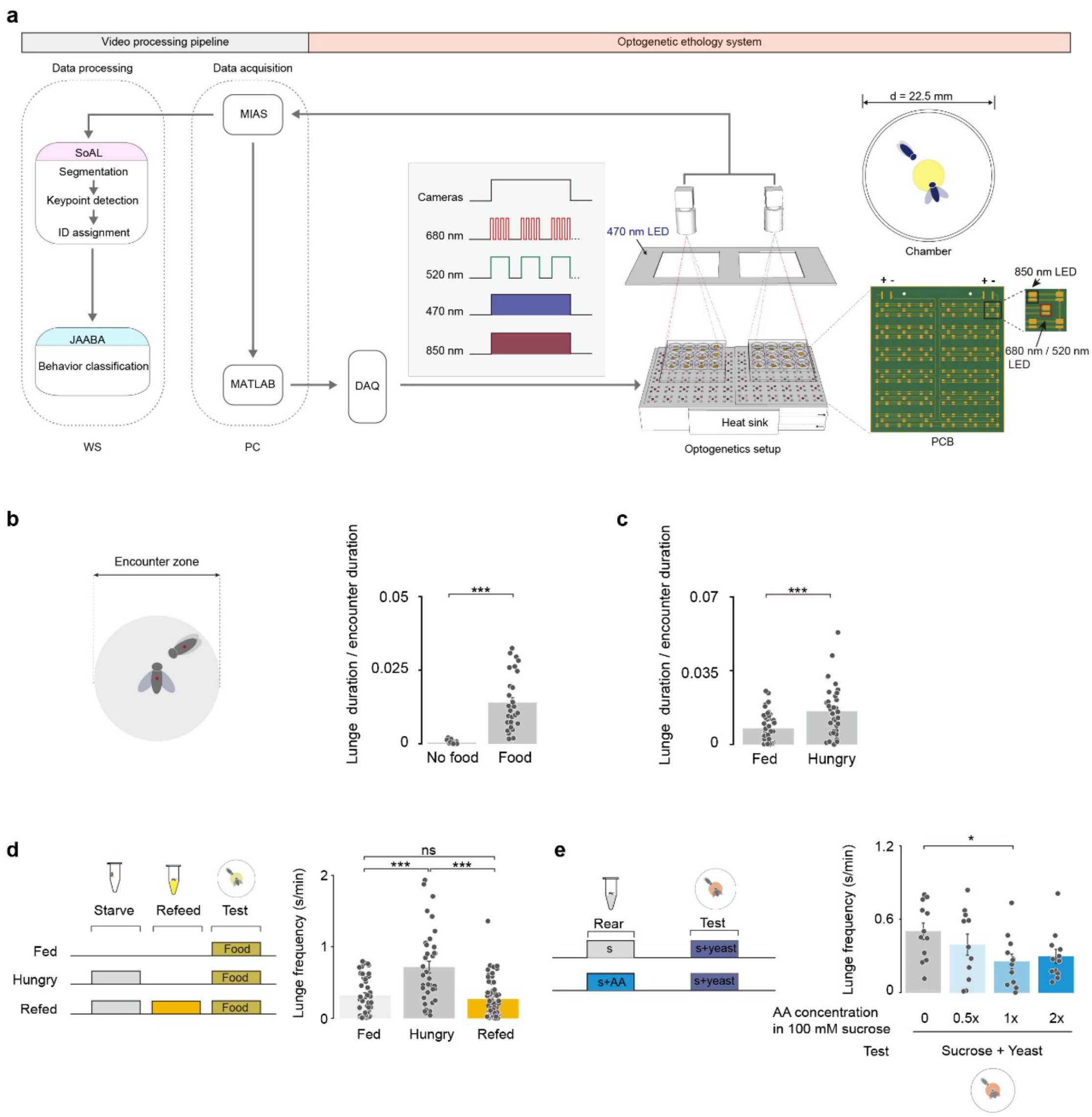

Supplementary Fig. 1 Additional data supporting food and hunger affect inter-male aggression.

a, Schematic of optogenetic ethology system (right) setup and video processing pipeline (left). See also Methods.

b, Left: Schematic of the encounter zone between two males. The gray-shaded circle represents the encounter zone, defined as a maximum distance of 6 mm (approximately two body lengths) between the centroids of the interacting males. Right: Ratio of lunge duration to encounter duration for wild-type males in chambers without or with food. See also Fig. 1c.

c, Ratio of lunge duration to encounter duration for wild-type males, reared with or without food, tested in chambers containing apple juice food. See also Fig. 1d.

d, Lunge frequencies of wild-type males interacting in chambers containing apple juice food under fed, hungry, and hungry then refed states. Same data as Fig. 1d.

e, Lunge frequencies of wild-type males reared on 100 mM sucrose (s) supplemented with increasing concentrations of amino acid (AA) mixture (0, 0.5×, 1×, 2×), followed by interactions on the same sucrose-yeast food.

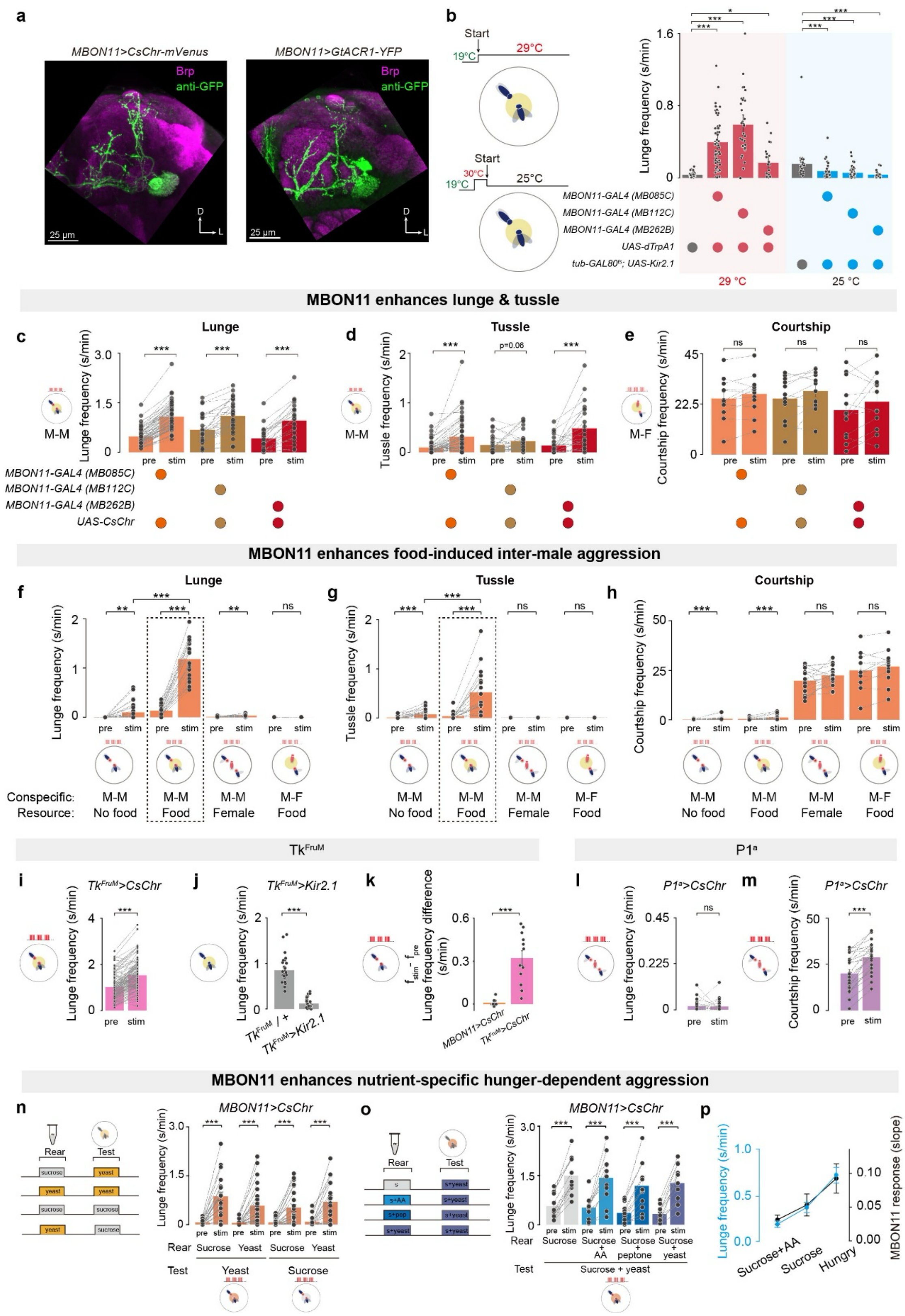

Supplementary Fig. 2 MBON11 mediates food-induced nutrient-specific-hunger-dependent inter-male aggression.

a, Confocal photomicrographs of the right hemispheric MBON11 expressing CsChrimson (left) and GtACR1 (right), visualized with anti-GFP (green) and

counterstained with anti-Brp (magenta) to label all synapses. Scale bars are 25 μm. See Methods and Supplementary Table 1 for details of all genotypes.
b, Schematics (left) and lunge frequencies (right) upon MBON11 thermogenetic stimulation using 3 different split-GAL4 drivers, alongside controls.
c-e, Lunge, tussle and courtship frequencies before (pre) and during (stim) MBON11 photoactivation using 3 different split-GAL4 drivers. Partial data in c same as Fig. 2a.
f-h, Lunge (f), tussle (g) and courtship (h) frequencies before (pre) and during (stim) MBON11 photoactivation under 4 conspecific context and resource combinations, including chambers with male conspecific (M-M) but no food (1^{st} condition), with male conspecific (M-M) and food (2^{nd} condition), with male conspecific (M-M) and tethered female as resource (3^{rd} condition), with free female conspecific (M-F) and food (4^{th} condition). MBON11 activation enhances food-induced inter-male lunge and tussle, highlighted by dashed boxes. Partial data in f same as Fig. 2b, partial data in h same as panel 2e.
i, Inter-male lunge frequencies before (pre) and during (stim) Tk^{FruM} photoactivation.
j, Lunge frequencies of interacting transgenic flies with Tk^{FruM} silenced by Kir2.1, alongside control.
k, Lunge frequency differences between during and before photoactivation of MBON11 or Tk^{FruM} in chambers without food.
l-m, Frequencies of male-male lunge (l) and male-female courtship (m) before (pre) and during (stim) $P1^a$ photoactivation by CsChrimson in males interacting with a male in chambers without food but with a live tethered female.
n, Lunge frequencies in nutrient-specific food value assay (schematic on the left), between males before (pre) and during (stim) MBON11 photoactivation by CsChrimson. Same data as Fig. 2d.
o, Lunge frequencies in protein-hunger assay (schematic on the left), between males before (pre) and during (stim) MBON11 photoactivation by CsChrimson. Same data as Fig. 2f.
p, Comparison between lunge frequencies (blue) and MBON11 calcium responses (black) across 3 rearing conditions, including sucrose supplemented with amino acid mixture (sucrose + AA), sucrose, and complete starvation (hungry). Same behavior data as Fig. 1d, f and same imaging data as Fig. 2j-k.

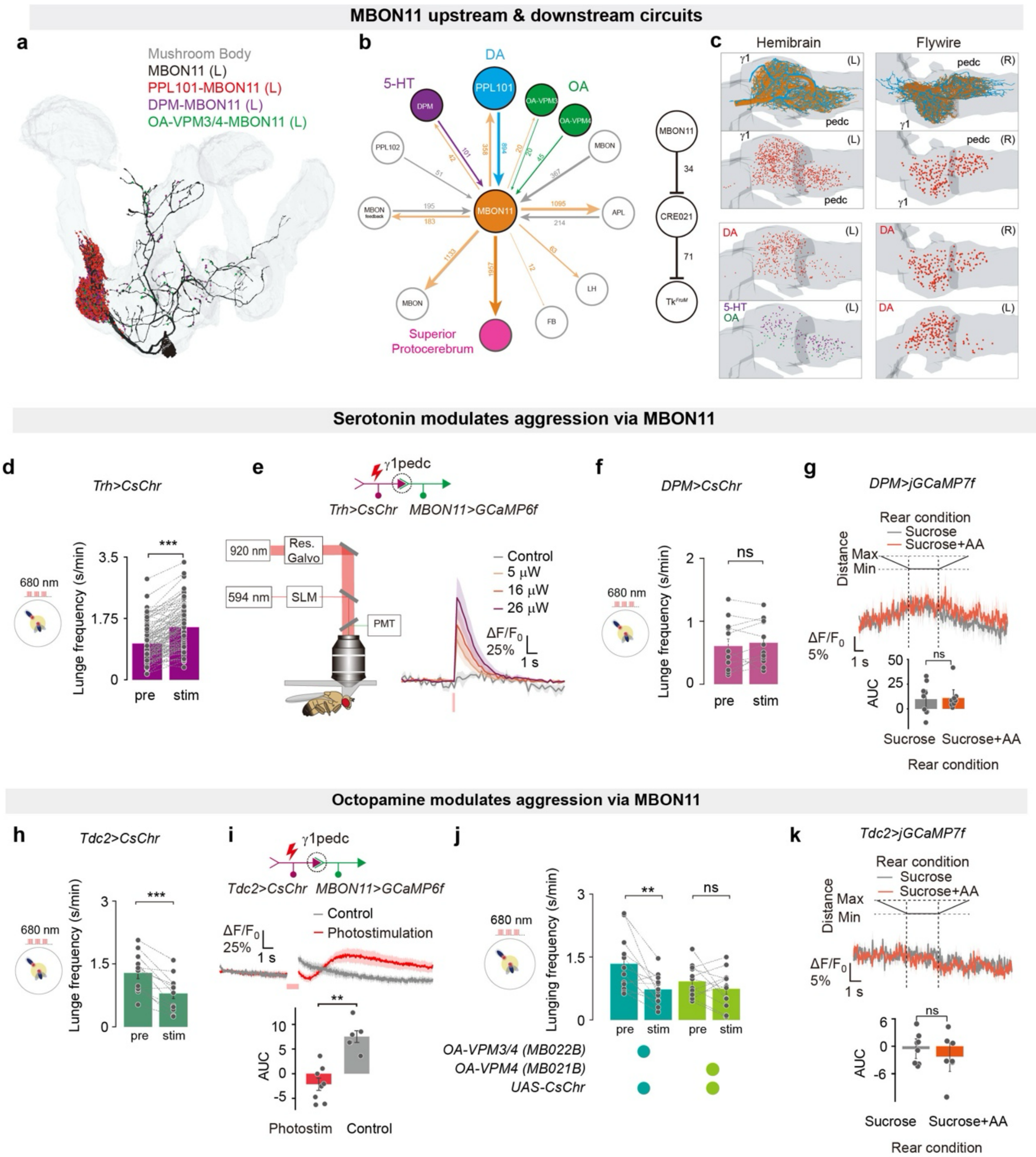

Supplementary Fig. 3 Aminergic neurons modulate MBON11 for aggression.

a, Volumetric reconstruction of an MBON11 neuron from hemibrain EM connectome, labeled with its major dopaminergic (red dots), serotonergic (purple dots), and octopaminergic (green dots) input synapses. Light gray shades outline the mushroom body. Also see Fig. 3a.

b, Left panel, major upstream and downstream neurons of MBON11 from FlyWire EM connectome, excluding kenyon cells. Line widths are related to the logarithm of the synapse counts (see Methods), which are labeled next to each arrow. FB, fan-shaped body; LH, lateral horn. Right panel, MBON11 to Tk^{FruM} connectivity via CRE021 in male-cns EM connectome. CRE021 is predicted as GABAergic, forming a disinhibition circuit together with GABAergic MBON11. Synapse counts are labeled next to each connection.

c, Upper four panels: volumetric reconstruction of densely innervated PPL101 axons (blue) and MBON11 dendrites (orange) in the γ1 and pedc compartments, labeled with PPL101-MBON11 synapses (red dots, second row). Lower four panels: PPL101-MBON11 (ipsilateral) synapses in γ1 and pedc compartments, predicted as dopaminergic (red), serotonergic (purple), and octopaminergic (green) (see Methods). Left and right columns are neurons from the hemibrain and FlyWire datasets, respectively.
d, Lunge frequencies before (pre) and during (stim) photoactivation of 5-HT neurons (labeled by Trh-GAL4) using CsChrimson in interacting transgenic males.
e, MBON11 calcium responses upon 5-HT neuron photoactivation at different intensities and control. Photoactivation of 5-HT neurons is restricted to the MB horizontal lobe using holographic photostimulation in head-fixed males (schematic). Red ticks denote photoactivation pulses.
f, Lunge frequencies before (pre) and during (stim) DPM neuron photoactivation using CsChrimson in interacting transgenic males.
g, DPM calcium response dynamics (upper) and magnitudes (AUC, lower) to solid sucrose-yeast food stimulation in males reared on sucrose or sucrose supplemented with amino acid mixture, using motorized solid food delivery (see Methods).
h, Lunge frequencies before (pre) and during (stim) octopaminergic neuron (labeled by Tdc2-GAL4) photoactivation with CsChrimson in interacting transgenic males.
i, MBON11 calcium response dynamics (upper) and magnitudes (lower) upon one-photon activation of Tdc2 using CsChrimson or control.
j, Lunge frequencies in interacting transgenic males before (pre) and during (stim) OA-VPM3/4 neuron photoactivation using CsChrimson.
k, Tdc2 calcium response dynamics (upper) and magnitudes (AUC, lower) to solid sucrose-yeast food stimulation males reared on sucrose or sucrose supplemented with amino acid mixture.

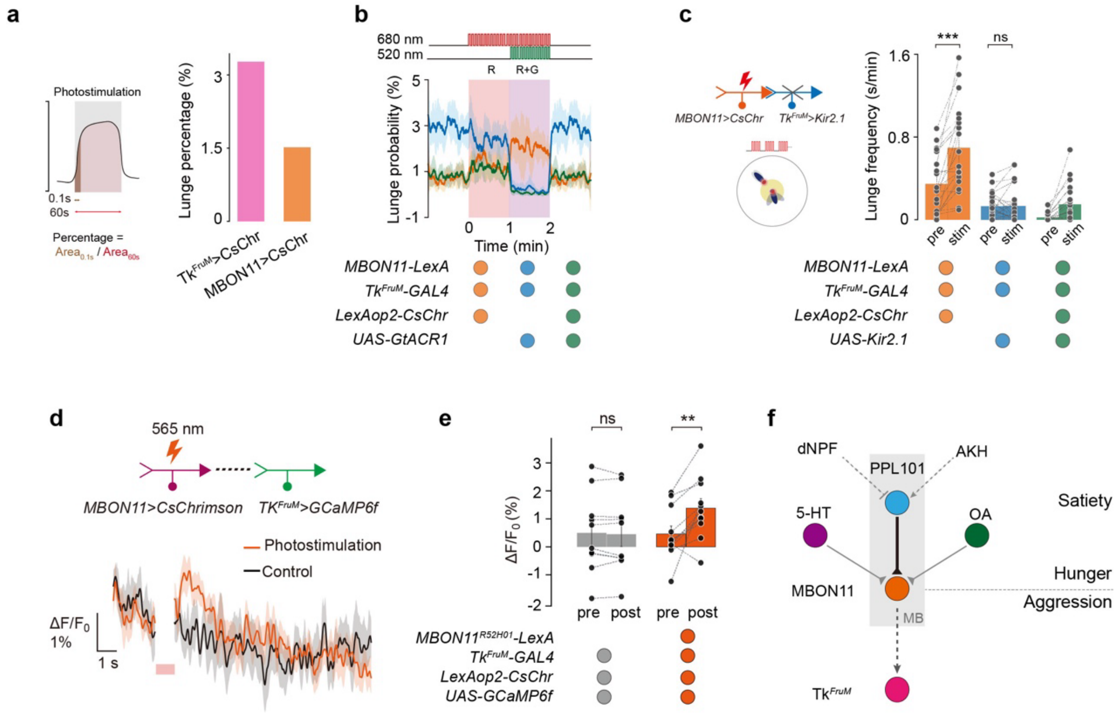

Supplementary Fig. 4 MBON11 modulates aggression via Tk^{FruM}.

a, Percentages of lunge durations during the first 100 ms over the entire 60 s photoactivation of Tk^{FruM} (pink) or MBON11 (orange) using CsChrimson. Same dataset as Fig. 2a and Supplementary Fig. 2i.

b, Mean lunge probability dynamics between interacting transgenic males with MBON11 photoactivation using CsChrimson, followed by additional Tk^{FruM} photoinhibition using GtACR1 (green line), compared to MBON11 photoactivation (orange line) or Tk^{FruM} photoinhibition (pink line) alone. Same data as Fig. 4g.

c, Lunge frequencies between interacting transgenic males before (pre) and during (stim) MBON11 photoactivation by CsChrimson when silencing Tk^{FruM} by Kir2.1 (green), compared to MBON11 photoactivation (orange) or Tk^{FruM} silencing (blue) alone.

d-e, Tk^{FruM} calcium response dynamics (d) and amplitudes (e) before (pre) and after (post) one-photon activation of MBON11 using CsChrimson or control.

f, Working model of a multilayer circuit for hunger-dependent aggression. Orexigenic dNPF and anorexigenic AKH neurons inhibits or excites dopaminergic PPL101 neuron to signal satiety, which is connected to “hangry” neuron MBON11 in the mushroom body, and finally to aggression neuron Tk^{FruM}. MBON11 is also positively and negatively modulated by serotonergic (5-HT) and octopaminergic (OA) neurons respectively for aggression.

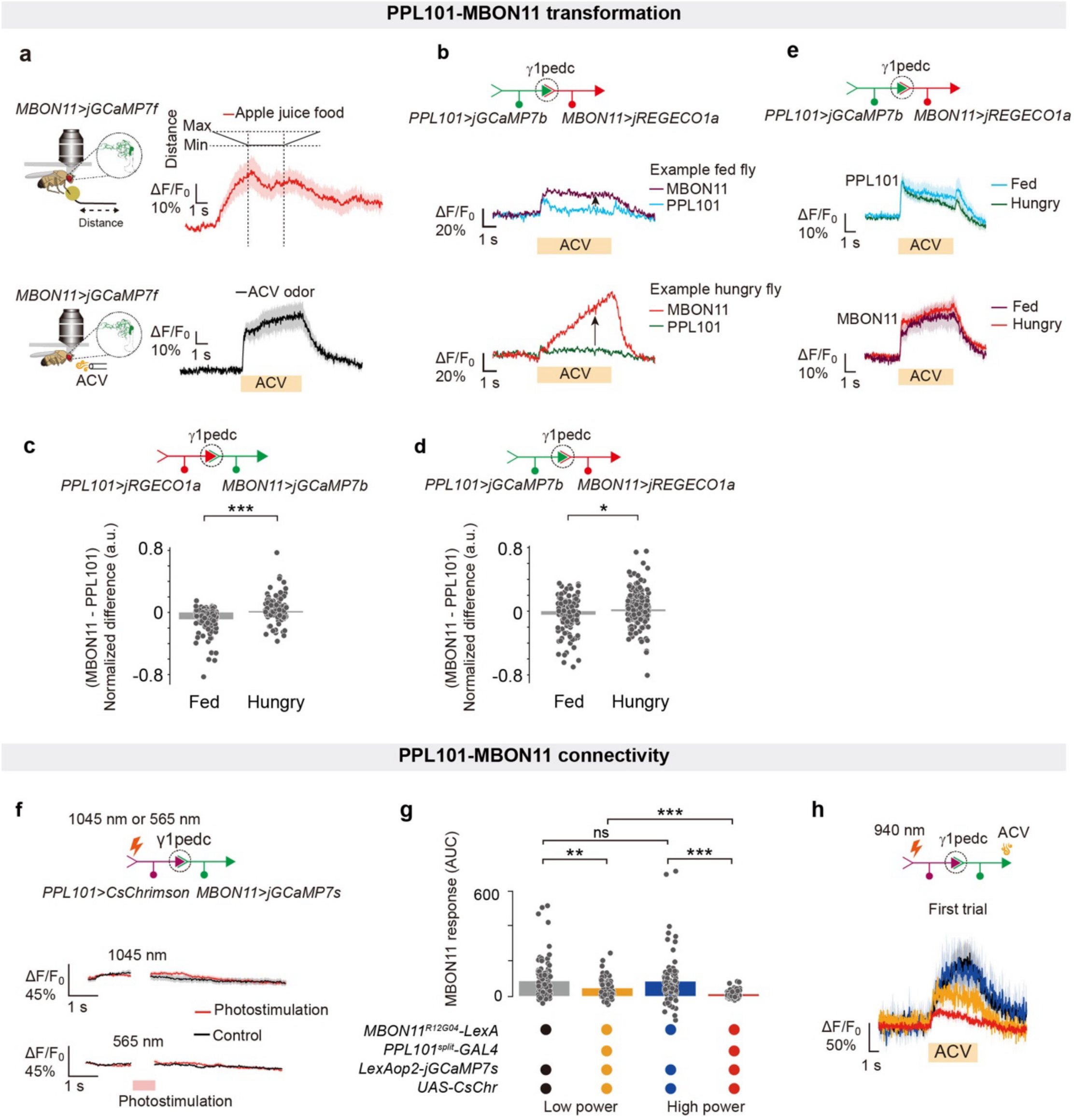

Supplementary Fig. 5 Additional data supporting PPL101 and MBON11 oppositely signal hunger.

a, Upper left, schematic for two-photon calcium imaging of MBON11 in head and proboscis fixed males with free legs to better simulate fly-food interaction, using motorized solid food delivery (see Methods). Insets show MBON11 skeleton (green) in the mushroom body (solid black line). Upper right, MBON11 calcium response dynamics with apple juice food stimulation (same dataset as Fig. 2i). Lower left, schematic for two-photon calcium imaging of MBON11 in head and leg fixed males with ACV odor stimulation. Insets show MBON11 (green) skeletons in the mushroom body (solid black line). Lower right, MBON11 response dynamics to ACV odor stimulation. The orange shadow denotes the odor stimulation period, same as follows. Same data as Fig. 8i.

b, Example PPL101 and MBON11 calcium response dynamics in the same dendritic compartment using dual-color imaging in fed (upper) and hungry (lower) males.

Black arrows denote MBON11-PPL101 activity difference, orange shadows denote the ACV odor stimulation period, same as follows. Also see Fig. 5b.
c-d, Normalized peak activity difference between MBON11 and PPL101 in fed and hungry males using dual-color imaging with two combinations of green and red calcium sensors.
e, Mean PPL101 (upper) and MBON11 (lower) calcium responses to ACV odor stimulation in fed and hungry males using dual-color imaging. Also see Fig. 5c-e.
f, MBON11 calcium responses upon two-photon (upper) or one-photon (lower) photoactivation of PPL101 using CsChrimson. No significant change was detectable in MBON11 responses upon PPL101 photoactivation in either condition.
g, MBON11 calcium response magnitudes (AUC) to ACV stimulation during simultaneous PPL101 two-photon photoactivation, including no PPL101 activation low imaging power (20 mW) control (black), no PPL101 activation high imaging power (40 mW) control (blue), low power PPL101 activation (orange), high power PPL101 activation (red). See Fig. 5i for the response dynamics.
h, First-trial MBON11 calcium response dynamics to ACV stimulation during simultaneous PPL101 two-photon photoactivation, including no PPL101 activation low power imaging (20 mW) control (black line), no PPL101 activation in high power imaging (40 mW) control (blue line), low power PPL101 activation (orange line), and high power PPL101 activation (red line). Same color code as panel g.

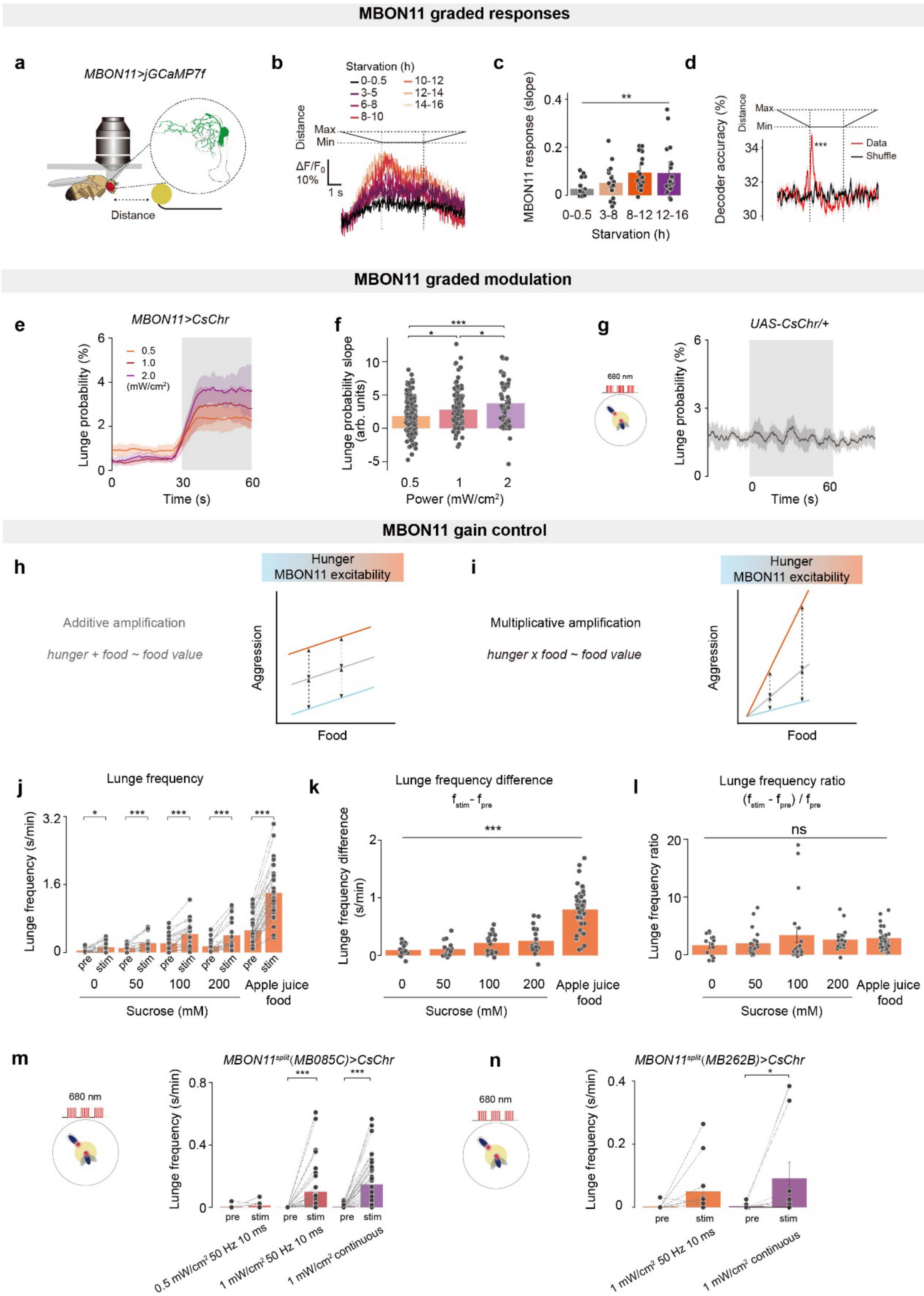

Supplementary Fig. 6 MBON11 amplifies food value for graded aggression modulation.

a-b, MBON11 calcium responses dynamics to apple juice food stimulation with seven categories of increasing starvation durations in head, legs, and proboscis fixed males, using motorized solid food delivery (see Methods). See also Fig. 6f.

c, MBON11 response slopes to apple juice food with increasing starvation durations. (same data as panel b, binned into four categories of starvation durations.)
d, Support vector machine (SVM) decoding of the four starvation duration categories over time, based on MBON11 calcium responses. The decoding accuracy is significantly higher compared to the shuffled data when approaching solid food. Same data as panel b, c.
e, Mean lunge probability rise dynamics upon MBON11 photoactivation with CsChrimson at intensities of 0.5, 1, or 2 mW/cm^2. Gray shadows denote photoactivation periods. Same data as Fig. 6h.
f, Slopes of mean lunge probability curves at the raise phase of various photoactivation intensities. Same data as Fig. 6h.
g, Lunge probability dynamics upon 680 nm photostimulation in UAS-CsChrimson/+ control males. Gray shadows denote photoactivation periods. Same data as Fig. 2a.
h-i, Hypothetical models of MBON11 amplification of food value for aggression modulation, including additive (h) and multiplicative (i) amplification models. In the additive amplification model (h), hunger (or MBON11 excitability) increases or decreases food-value-based aggression by a fixed amount regardless of the baseline aggression level. In the multiplicative amplification model (i), hunger (or MBON11 excitability) increases or decreases food-value-based aggression proportionally to the baseline aggression level.
j-l, Lunge frequencies (j), lunge frequency differences (k), and lunge frequency ratios (l) between males in chambers containing apple juice food which promotes aggression or foods with increasing concentrations of sucrose before (pre) and during (stim) MBON11 photoactivation. For ratio calculations, data with zero lunge frequency before stimulation are excluded in k and l. See Methods for the metrics. Same data as Fig. 6a, i.
m-n, Lunge frequencies between two males in chambers without food before (pre) and during (stim) MBON11 photoactivation of different photostimulation conditions using MB085C (m) and MB262B driver (n). Activating MBON11 in foodless chambers enhances lunge frequency only to a low level (m, 0.01 ± 0.01 s/min under 50 Hz of 10-ms pulse photoactivation at 0.5 mW/cm^2), even with continuous activation at higher intensity (m, 0.15 ± 0.03 s/min under 1 mW/cm^2 continuous photoactivation).

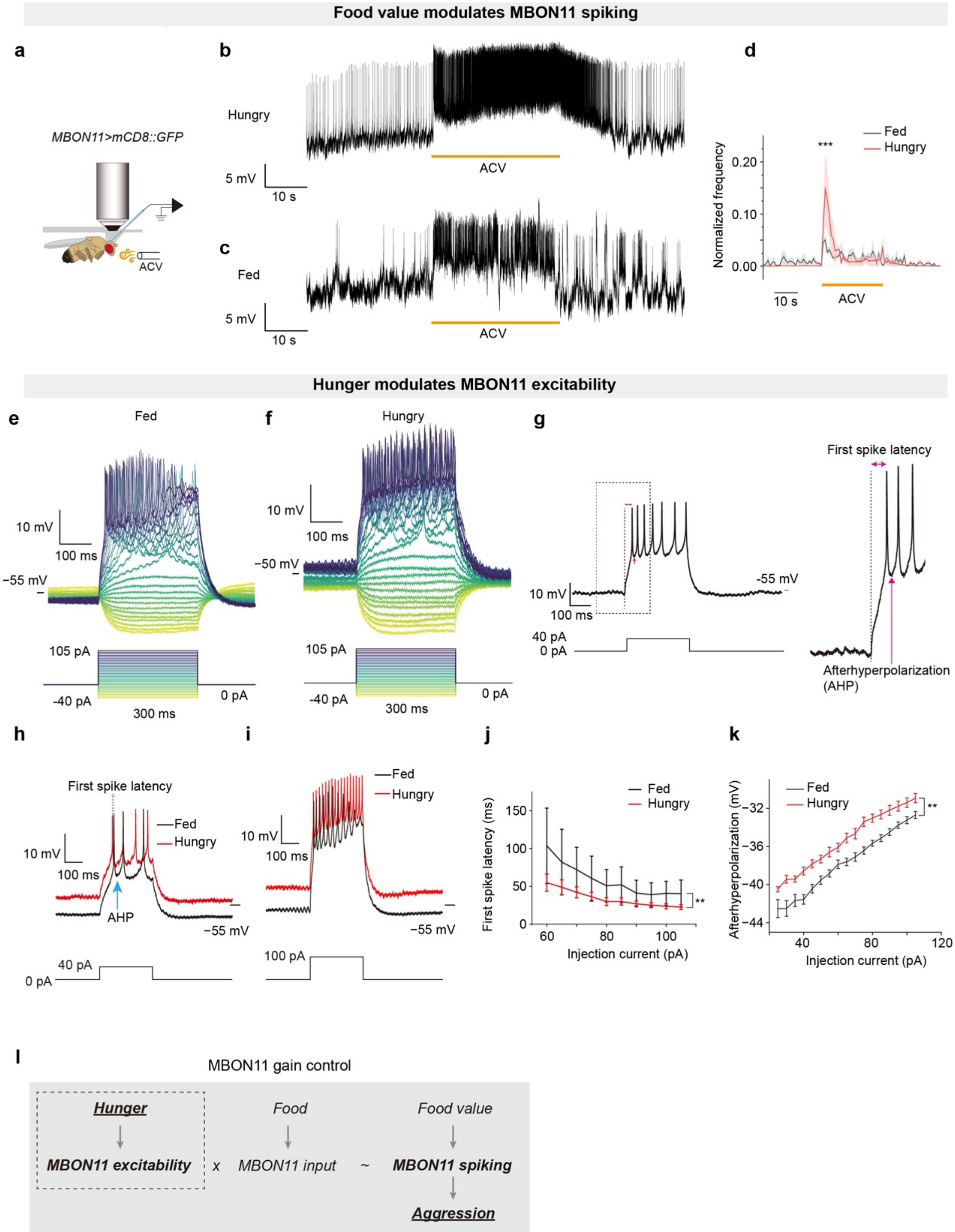

Supplementary Fig. 7 Hunger modulates MBON11 excitability.

a, Schematic for whole-cell patch-clamp recording of MBON11 *in vivo* during ACV food odor stimulation.

b-c, Example traces of MBON11 voltage responses to the ACV odor stimulation in hungry (b) or fed (c) males. Orange lines denote ACV stimulation periods.

d, Normalized firing rates of MOBN11 in response to the ACV odor stimulation in fed (black line) or hungry (red line) males. MBON11 firing rates in hungry males are

higher than that in fed males ($p < 0.001$). Orange lines denote ACV stimulation periods.
e-f, Example traces of MBON11 membrane potential in response to injected current steps from -40 pA to 105 pA, in fed (e) or hungry (f) males.
g, Example trace of the MBON11 membrane potential to a 40 pA current injection in a fed male. Zoomed-in view of the dashed rectangle shown on the right highlights the long first spike latency and large afterhyperpolarization (AHP, red arrows).
h-i, Example traces of MBON11 voltage responses to 40 pA (h) and 100 pA (i) current steps of 300 ms, in fed (black) or hungry (red) males. Longer first spike latency and larger afterhyperpolarization in fed males are highlighted (h, blue arrows). Also see Fig. 6n.
j-k, First spike latency (j) and afterhyperpolarization (AHP, k) of MOBN11 voltage responses to depolarizing current steps in fed (black) or hungry (red) males.
l, Working model of MBON11 multiplicative gain control via membrane excitability for hunger-dependent aggression modulation. Hunger (or optogenetic activation) modulates MBON11 excitability, which scales MBON11 synaptic input to tune its spiking, which in turn modulates aggression intensity, thereby relating hunger (upper left, underlined) to aggression (lower right, underlined) via cellular electrophysiology. Dashed box highlights how hunger modulates membrane excitability for gain control, the mechanism of which is examined in the rest of this study.

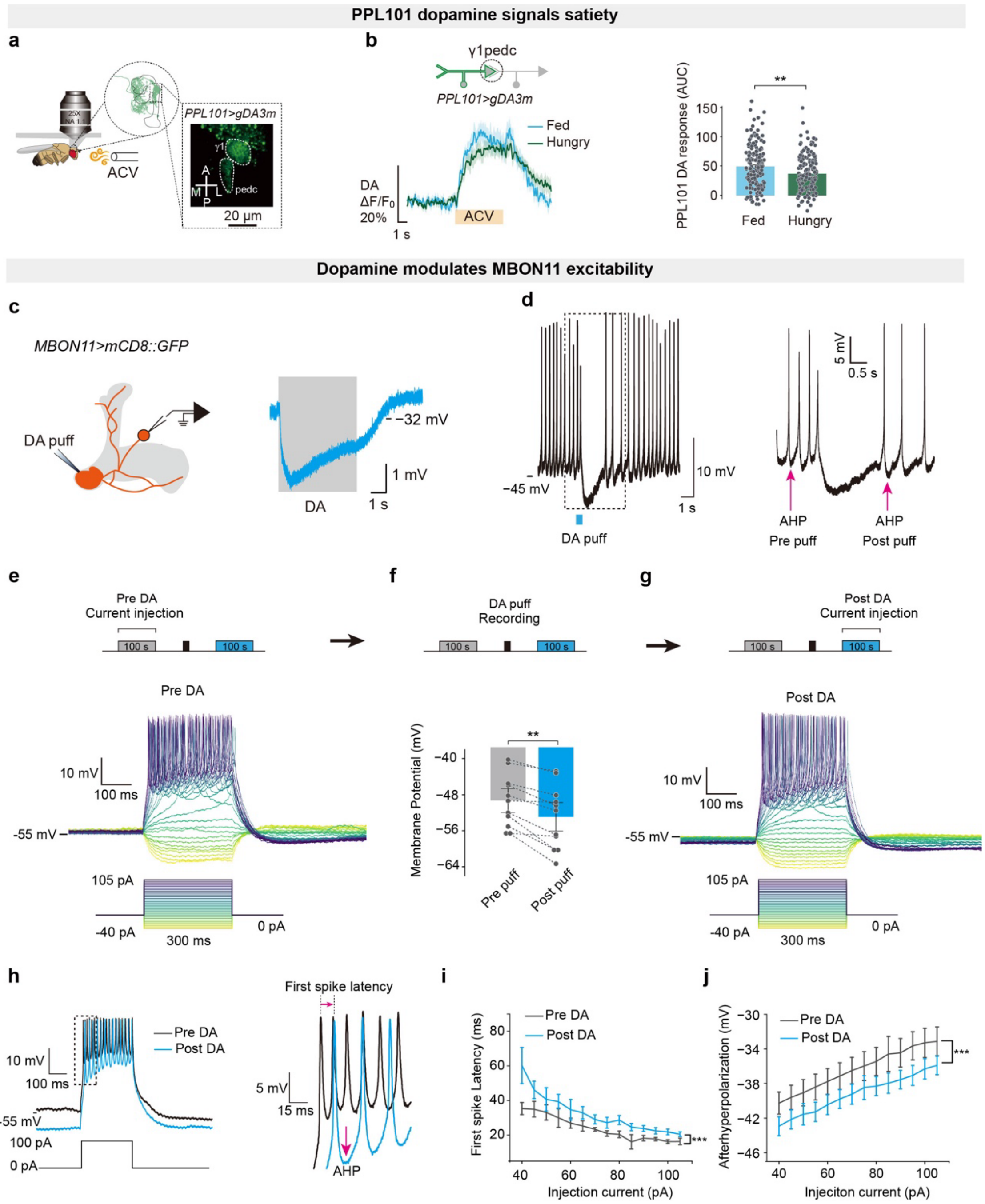

Supplementary Fig. 8 Additional data supporting PPL101 dopamine signals hunger states and modulates MBON11 excitability.

a, Schematic for two-photon dopamine imaging of PPL101 in head and leg fixed males with ACV odor stimulation. Insets show dorsal view PPL101 (green) skeleton in the mushroom body (solid black line) and transgenic fly fluorescence expression of gDA3m in PPL101, with γ1 and pedc compartments highlighted (white dashes).

b, PPL101 dopamine response dynamics (left) and magnitudes (right) to ACV odor stimulation in hungry (green) or fed (blue) conditions.

c, Left, schematic of whole-cell patch clamp recording on the MBON11 cell body during dopamine puffing in its dendritic compartment. Right, membrane potential trace of an MBON11 neuron upon a 5-s long dopamine puffing.
d, Membrane potential of MBON11 after a 500 ms puffing of 10 mM dopamine. Zoomed-in view of the dashed rectangle is shown on the right, highlighting larger afterhyperpolarization after dopamine puffing compared to that before (red arrows). Blue bar (left) denotes dopamine puffing.
e, g, Example traces of MBON11 membrane potential to current steps from -40 pA to 105 pA, before (e) and after (g) dopamine puffing. Schematics on top from e to g show the time and periods of current injection and recording during the course of the experiment. Post-puff current injection period and the preceding delay since puffing total over 100 seconds, necessitating persistent dopamine modulation.
f, Mean membrane potentials of MBON11 immediately before (Pre puff) and after (Post puff) dopamine puffing. Dots and bars denote individual males and their means, respectively. Schematic on top show the time point of recording during the course of the experiment.
h, Example traces of MBON11 voltage responses to 300 ms of 100 pA current injection, before (black) and after (blue) dopamine puffing on the same cell. Zoomed-in view of the dashed rectangle (shown on the right) highlights the longer first spike latency and larger afterhyperpolarization (red arrows) after dopamine puffing. Post-puff current injection begins 221 s after puffing ends, indicating persistent dopamine modulation.
i-j, First spike latency (i) and afterhyperpolarization (j) of MOBN11 voltage responses to depolarizing current steps before (black) and after (blue) dopamine puffing. Dopamine modulates latency and AHP across all currents injected over the 100-s period, indicating persistence.

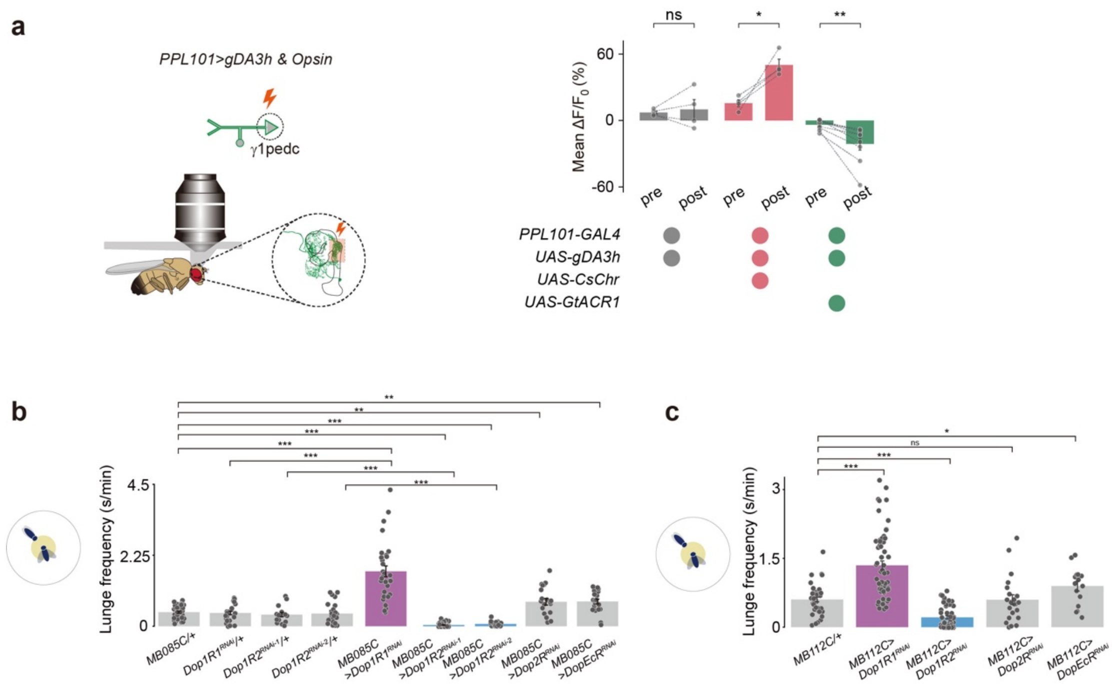

Supplementary Fig. 9 Opposing dopamine release and opposing dopamine receptors for aggression modulation.

a, Schematics (left) and magnitudes (right) of PPL101 dopamine responses before (pre) and immediately after (post) two-photon CsChrimson photoactivation or two-photon GtACR1 photoinhibition, respectively. See Fig. 7n for response dynamics.

b-c, Lunge frequencies in food chambers between transgenic males with dopamine receptor subtype knockdown via RNA interference in MBON11, using split-GAL4 driver MB085C (b) or MB112C (c). We tested two different RNAi effector stocks for Dop1R2 knockdown (see Supplementary Table 1 for details). Results for Dop1R1 and Dop1R2 RNAi are highlighted in purple and blue, respectively.

MB085C>Dop1R1^{RNAi}, MB085C>Dop1R2^{RNAi-1}, MB085C / +, Dop1R1^{RNAi} / + and Dop1R2^{RNAi-1} / + results are also displayed in Fig. 7o.

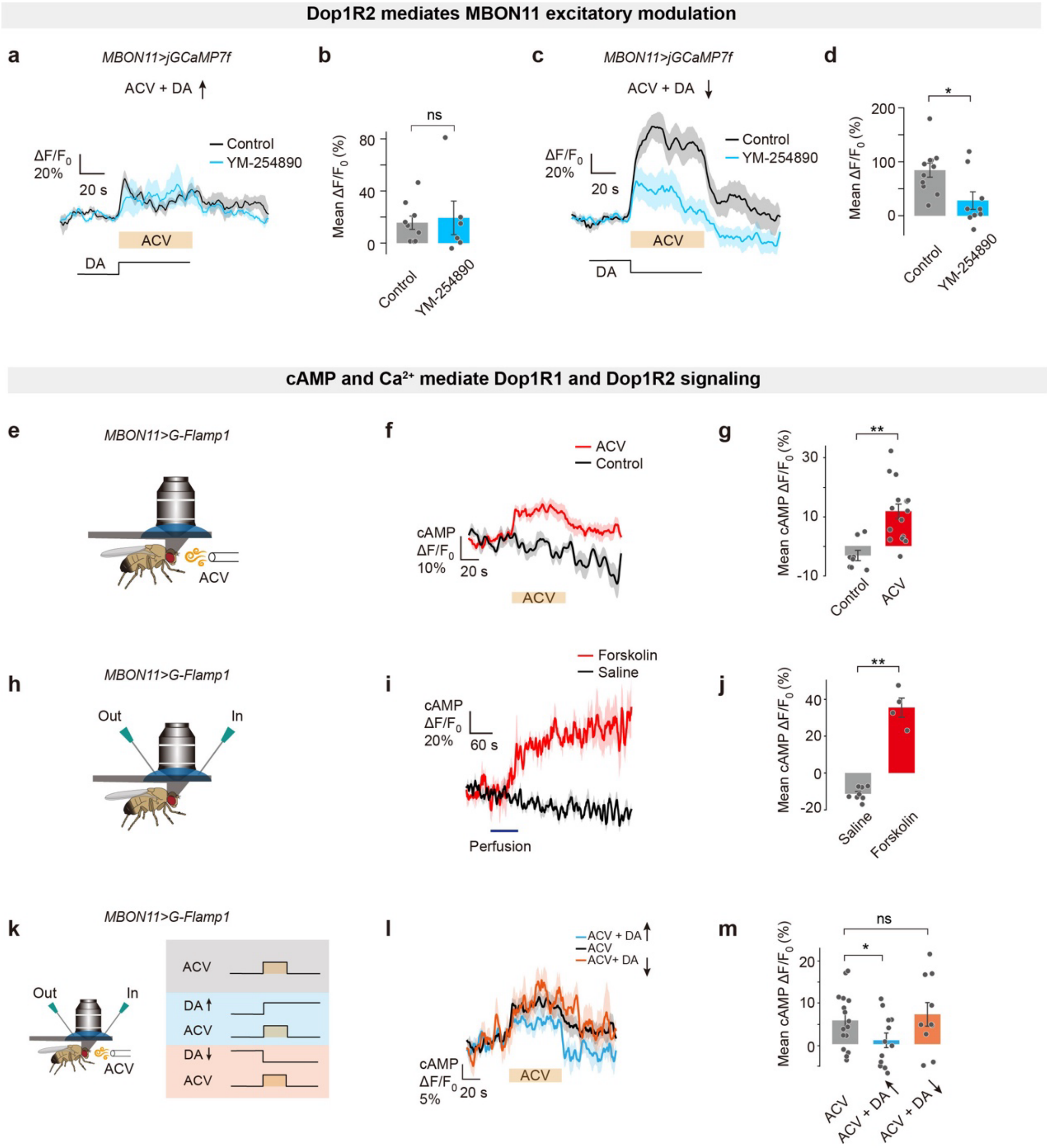

Supplementary Fig. 10 Additional data supporting opposing dopamine pathways mediate hunger-dependent aggression.

a-b, MBON11 response dynamics (a) and magnitudes (b) in males to ACV food odor stimulation when perfusing increasing concentrations of dopamine with (blue) or without (black, control) 1 μM of Gαq inhibitor YM-254890. Control is the same data as Fig. 8b-c.

c-d, MBON11 response dynamics (c) and magnitudes (d) in males to ACV food odor stimulation when perfusing decreasing concentrations of dopamine with (blue) or without (black, control) 1 μM of Gαq inhibitor YM-254890. Control is the same data as Fig. 8b-c.

e-g, MBON11 cAMP response dynamics (f) and magnitudes (g) to ACV food odor stimulation, compared to no odor control.

h-j, MBON11 first-trial cAMP response dynamics (i) and magnitudes (j) when perfusing 100 μM of adenylyl cyclase activator forskolin, compared to saline control. k-m, MBON11 cAMP response dynamics (l) and magnitudes (odor off periods, m) to food odor stimulation alone (black), food odor stimulation with dopamine increase (blue), and food odor stimulation with dopamine decrease (orange). Control is the same data as ACV odor response in panel f.

Supplementary Table 1

Full genotypes of flies used to generate data presented in each figure.

Figure	**Genotype**	**Abbreviation**
Fig. 1		
Fig. 1b	Canton-S	WT
Fig. 1c	Canton-S	WT
Fig. 1d	Canton-S	WT
Fig. 1e	Canton-S	WT
Fig. 1f	Canton-S	WT
Fig. 2		
Fig. 2a	20 x UAS-CsChrimson-mVenus @attP18; + / +; + / +	CsChr / +
	+; + / +; R52H01-AD @VK00027, R52B07-DBD @attP2 / +	MB085C / +
	+; + / +; R93D10-AD @VK00027, R13F04-DBD @attP2 / +	MB112C / +
	+; R52B07-AD @attP40 / +; R52H01-DBD @attP2 / +	MB262B / +
	20 x UAS-CsChrimson-mVenus @attP18; + / +; R52H01-AD @VK00027, R52B07-DBD @attP2 / +	MB085C > CsChr
	20 x UAS-CsChrimson-mVenus @attP18; + / +; R93D10-AD @VK00027, R13F04-DBD @attP2 / +	MB112C > CsChr
	20 x UAS-CsChrimson-mVenus @attP18; R52B07-AD @attP40 / +; R52H01-DBD @attP2 / +	MB262B > CsChr
	+; + / +; 20 x UAS-GtACR1-YFP @attP2 / +	GtACR1 / +
	+; + / +; R52H01-AD @VK00027, R52B07-DBD @attP2 / 20 x UAS-GtACR1-YFP @attP2	MB085C > GtACR1
	+; R52B07-AD @attP40 / +; R52H01-DBD @attP2 / 20 x UAS-GtACR1-YFP @attP2	MB262B > GtACR1
	+; + / +; R93D10-AD @VK00027, R13F04-DBD @attP2 / 20 x UAS-GtACR1-YFP @attP2	MB112C > GtACR1
Fig. 2b-c	20 x UAS-CsChrimson-mVenus @attP18; + / +; R52H01-AD @VK00027, R52B07-DBD @attP2 / +	MBON11 > CsChr
Fig. 2d	20 x UAS-CsChrimson-mVenus @attP18; + / +; R52H01-AD @VK00027, R52B07-DBD @attP2 / +	MBON11 > CsChr

Fig. 2e	+; + / +; R52H01-AD @VK00027, R52B07-DBD @attP2 / UAS-Kir2.1-eGFP @attP2	MBON11 > Kir2.1
Fig. 2f	20 x UAS-CsChrimson-mVenus @attP18; + / +; R52H01-AD @VK00027, R52B07-DBD @attP2 / +	MBON11 > CsChr
Fig. 2g	+; + / +; R52H01-AD @VK00027, R52B07-DBD @attP2 / UAS-Kir2.1-eGFP @attP2	MBON11 > Kir2.1
Fig. 2h-k	+; + / +; R52H01-AD @VK00027, R52B07-DBD @attP2 / 20 x UAS-jGCaMP7f @VK00005	MBON11 > jGCaMP7f
Fig. 3		
Fig. 3d	+; + / +; 20 x UAS-GtACR1-YFP @attP2 / +	GtACR1 / +
	+; R52H03-AD @attP40 / +; R14E06-DBD @attP2 / +	MB502B / +
	+; R52H03-AD @attP40 / +; R14E06-DBD @attP2 / 20 x UAS-GtACR1-YFP @attP2	MB502B > GtACR1
	+; ple-AD @attP40 / +; R22B12-DBD @attP2 / 20 x UAS-GtACR1-YFP @attP2	MB320C > GtACR1
	+; R30E11-AD @attP40 / +; R22B12-DBD @attP2 / 20 x UAS-GtACR1-YFP @attP2	MB438B > GtACR1
Fig. 3e	+; ple-AD @attP40 / +; R22B12-DBD @attP2 / +	PPL101 / +
	20 x UAS-CsChrimson-mVenus @attP18; + / +; + / +	CsChr / +
	20 x UAS-CsChrimson-mVenus @attP18; ple-AD @attP40 / +; R22B12-DBD @attP2 / +	PPL101 > CsChr
Fig. 3f	+; ple-AD @attP40 / +; R22B12-DBD @attP2 / +	PPL101 / +
	+; UAS-nz::caspase3 @VIE-19a, UAS-caspase3::cz @VIE-260b / +; + / +	Caspase-3 / +
	+; UAS-IVS-grim-WPRE @su(Hw)attP6 / +; UAS-reaper / +	Reaper & Grim / +
	+; ple-AD @attP40 / UAS-nz::caspase3 @VIE-19a, UAS-caspase3::cz @VIE-260b; R22B12-DBD @attP2 / +	PPL101 > Caspase-3
	+; ple-AD @attP40 / UAS-IVS-grim-WPRE @su(Hw)attP6; R22B12-DBD @attP2 / UAS-reaper	PPL101 > Reaper & Grim

Fig. 3g-i	+; 20 x UAS-jGCaMP7f @su(Hw)attP5 / +; ple-AD @VK00027, R22B12-DBD @attP2 / +	PPL101 > jGCaMP7f
Fig. 4		
Fig. 4b	+; 20 x UAS-GtACR1-YFP @attP2 / +; + / +	GtACR1 / +
	+; R52H03-AD @attP40 / +; R14E06-DBD @attP2 / +	PPL101 / +
	+; + / +; R52H01-AD @VK00027, R52B07-DBD @attP2 / +	MBON11/ +
	+; R52H03-AD @attP40 / 20 x UAS-GtACR1-YFP @attP2; R14E06-DBD @attP2 / +	PPL101 > GtACR1
	+; 20 x UAS-GtACR1-YFP @attP2 / +; R52H01-AD @VK00027, R52B07-DBD @attP2 / +	MBON11 > GtACR1
	+; R52H03-AD @attP40 / 20 x UAS-GtACR1-YFP @attP2; R52H01-AD @VK00027, R52B07-DBD @attP2 / R14E06-DBD @attP2	MBON11 > GtACR1 & PPL101 > GtACR1
Fig. 4d	13 x LexAop2-CsChrimson-mVenus @attP18; + / +; + / +	CsChr / +
	+; + / +; UAS-Kir2.1-eGFP @attP2 / +	Kir2.1/ +
	+; R12G04-LexA::p65 / +; R22B12-DBD @attP2, ple-AD @VK00027 / +	PPL101; MBON11 / +
	13 x LexAop2-CsChrimson-mVenus @attP18; + / +; UAS-Kir2.1-eGFP @attP2 / +	CsChr; Kir2.1 / +
	13 x LexAop2-CsChrimson-mVenus @attP18; R12G04-LexA::p65 / +; R22B12-DBD @attP2, ple-AD @VK00027 / +	PPL101 > empty & MBON11 > CsChr
	+; R12G04-LexA::p65 / +; R22B12-DBD @attP2, ple-AD @VK00027 / UAS-Kir2.1-eGFP @attP2	PPL101 > Kir2.1 & MBON11 > empty
	13 x LexAop2-CsChrimson-mVenus @attP18; R12G04-LexA::p65 / +; R22B12-DBD @attP2, ple-AD @VK00027 / UAS-Kir2.1-eGFP @attP2	PPL101 > Kir2.1 & MBON11 > CsChr
Fig. 4e	13 x LexAop2-CsChrimson-mVenus @attP18; R12G04-	PPL101 > empty & MBON11 > CsChr

	LexA::p65 / +; R22B12-DBD @attP2, ple-AD @VK00027 / +	
	13 x LexAop2-CsChrimson-mVenus @attP18; R12G04-LexA::p65 / +; R22B12-DBD @attP2, ple-AD @VK00027 / UAS-Kir2.1-eGFP @attP2	PPL101 > Kir2.1 & MBON11 > CsChr
Fig. 4g	+; + / +; 20 x UAS-GtACR1-YFP @attP2 / +	GtACR1 / +
	13 x LexAop2-CsChrimson-mVenus @attP18; + / +; + / +	CsChr / +
	13 x LexAop2-CsChrimson-mVenus @attP18; + / +; 20 x UAS-GtACR1-YFP @attP2 / +	CsChr; GtACR1 / +
	+; R52H01-LexA::p65 @attP40 / +; Tk^{FruM}-GAL4 @attP2 / +	MBON11; Tk^{FruM} / +
	13 x LexAop2-CsChrimson-mVenus @attP18; R52H01-LexA::p65 @attP40 / +; Tk^{FruM}-GAL4 @attP2 / +	MBON11 > CsChr & Tk^{FruM} > empty
	w-; R52H01-LexA::p65 @attP40 / +; Tk^{FruM}-GAL4 / 20 x UAS-GtACR1-YFP @attP2	MBON11 > empty & Tk^{FruM} > GtACR1
	13 x LexAop2-CsChrimson-mVenus @attP18; R52H01-LexA::p65 @attP40 / +; Tk^{FruM}-GAL4 @attP2 / 20 x UAS-GtACR1-YFP @attP2	MBON11 > CsChr & Tk^{FruM} > GtACR1
Fig. 5		
Fig. 5a	13 x LexAop2-jGCaMP7b @su(Hw)attP8; R14E06-LexA @attP40 / +; R52H01-AD @VK00027, R52B07-DBD @attP2 / 20 x UAS-jRGECO1a @VK00005	PPL101 > jGCaMP7b & MBON11 > jRGECO1a
Fig. 5b-d	13 x LexAop2-jGCaMP7b @su(Hw)attP8; R12G04-LexA @attP40 / +; ple-AD @VK00027, R22B12-DBD @attP2 / 20x UAS-jRGECO1a @VK00005	MBON11 > jGCaMP7b & PPL101 > jRGECO1a
Fig. 5e	13 x LexAop2-jGCaMP7b @su(Hw)attP8; R14E06-LexA @attP40 / +; R52H01-AD @VK00027, R52B07-DBD @attP2 / 20 x UAS-jRGECO1a @VK00005	PPL101 > jGCaMP7b & MBON11 > jRGECO1a
Fig. 5f-g	+; + / +; R52H01-AD @VK00027, R52B07-DBD @attP2 / 20 x UAS-jGCaMP7f @VK00005	MBON11 > jGCaMP7f

Fig. 5i	+; R12G04-LexA @attP40 / R52H03-AD @attP40; 20 x UAS-CsChrimson.mCherry @su(Hw)attP1, 13 x LexAop2-IVS-Syn21-jGCaMP7s-p10 @VK00005 / R14E06-DBD @attP2	PPL101 > CsChr & MBON11 > jGCaMP7s
Fig. 5i	+; R12G04-LexA @attP40 / +; 20 x UAS-CsChrimson.mCherry @su(Hw)attP1, 13 x LexAop2-IVS-Syn21-jGCaMP7s-p10 @VK00005	empty > CsChr & MBON11 > jGCaMP7s
Fig. 6		
Fig. 6a	Canton-S	WT
Fig. 6a	20 x UAS-CsChrimson-mVenus @attP18; + / +; R52H01-AD @VK00027, R52B07-DBD @attP2 / +	MBON11 > CsChr
Fig. 6c	Canton-S	WT
Fig. 6c	20 x UAS-CsChrimson-mVenus @attP18; + / +; R52H01-AD @VK00027, R52B07-DBD @attP2 / +	MBON11 > CsChr
Fig. 6c	+; + / +; R52H01-AD @VK00027, R52B07-DBD @attP2 / UAS-Kir2.1-eGFP @attP2	MBON11 > Kir2.1
Fig. 6f-g	+; + / +; R52H01-AD @VK00027, R52B07-DBD @attP2 / 20 x UAS-jGCaMP7f @VK00005	MBON11 > jGCaMP7f
Fig. 6h	20 x UAS-CsChrimson-mVenus @attP18; + / +; R52H01-AD @VK00027, R52B07-DBD @attP2 / +	MBON11 > CsChr
Fig. 6i-j	20 x UAS-CsChrimson-mVenus @attP18; + / +; R52H01-AD @VK00027, R52B07-DBD @attP2 / +	MBON11 > CsChr
Fig. 6k	Canton-S	WT
Fig. 6m-o	10 x UAS-mCD8::GFP@su(Hw)attP8; + / +; R52H01-AD @VK00027, R52B07-DBD @attP2 / +	MBON11 > mCD8::GFP
Fig. 7		
Fig. 7a-c	+; + / +; ple-AD @VK00027, R22B12-DBD @attP2 / UAS-gDA3m @VK00005	PPL101 > gDA3m
Fig. 7d-e	+; UAS-gDA3h @attP40 / +; ple-AD @VK00027, R22B12-DBD	PPL101 > gDA3h

	@attP2 / +	
Fig. 7d-e	+; UAS-gDA3h @attP40 / +; ple-AD @VK00027, R22B12-DBD @attP2 / UAS-TH^{RNAi} @attP2	PPL101 > gDA3h & PPL101 > TH^{RNAi}
Fig. 7f-g	+; + / +; ple-AD @VK00027, R22B12-DBD @attP2 / UAS-gDA3m @VK00005	PPL101 > gDA3m
Fig. 7h-l	10 x UAS-mCD8::GFP@su(Hw)attP8; + / +; R52H01-AD @VK00027, R52B07-DBD @attP2 / +	MBON11 > mCD8::GFP
Fig. 7m	+; ple-AD @attP40 / +; R22B12-DBD @attP2 / +	PPL101 / +
	+; + / +; TH^{RNAi} / +	TH^{RNAi} / +
	+; ple-AD @attP40 / +; R22B12-DBD @attP2 / TH^{RNAi}	PPL101 > TH^{RNAi}
Fig. 7n	+; UAS-gDA3h @attP40 / +; ple-AD @VK00027, R22B12-DBD @attP2 / +	PPL101 > gDA3h
Fig. 7n	+; UAS-gDA3h @attP40 / +; ple-AD @VK00027, R22B12-DBD @attP2 / 20 x UAS-GtACR1-YFP @attP2	PPL101 > gDA3h & PPL101 > GtACR1
Fig. 7n	+; UAS-gDA3h @attP40 / +; ple-AD @VK00027, R22B12-DBD @attP2 / 20 x UAS-CsChrimson.mCherry @su(Hw)attP1	PPL101 > gDA3h & PPL101 > CsChr
Fig. 7o	+; + / +; R52H01-AD @VK00027, R52B07-DBD @attP2 / +	MBON11 / +
	+; Dop1R1^{RNAi} / +; + / +	Dop1R1^{RNAi} / +
	+; + / +; Dop1R2^{RNAi} / +	Dop1R2^{RNAi} / +
	+; Dop1R1^{RNAi} / +; R52H01-AD @VK00027, R52B07-DBD @attP2 / +	MBON11 > Dop1R1^{RNAi}
	+; + / +; R52H01-AD @VK00027, R52B07-DBD @attP2 / Dop1R2^{RNAi}	MBON11 > Dop1R2^{RNAi}
Fig. 8		
Fig. 8b-j	+; 20 x UAS-jGCaMP7f @su(Hw)attP5 / +; R52H01-AD @VK00027, R52B07-DBD @attP2 / +	MBON11 > jGCaMP7f
Fig. 8d-j	+; 20 x UAS-jGCaMP7f @su(Hw)attP5 / Dop1R1^{RNAi}	MBON11 > jGCaMP7f & MBON11 > Dop1R1^{RNAi}

	@attP40; R52H01-AD @VK00027, R52B07-DBD @attP2 / +	
Fig. 8d-j	+; 20 x UAS-jGCaMP7f @su(Hw)attP5 / +; R52H01-AD @VK00027, R52B07-DBD @attP2 / Dop1R2^{RNAi} @attP2	MBON11 > jGCaMP7f & MBON11 > Dop1R2^{RNAi}
Fig. 8k-m	+; 20 x UAS-G-Flamp1 @attP40 / +; R52H01-AD @VK00027, R52B07-DBD @attP2 / +	MBON11 > G-Flamp1
Fig. 8k-m	+; 20 x UAS-G-Flamp1 @attP40 / Dop1R1^{RNAi} @attP40; R52H01-AD @VK00027, R52B07-DBD @attP2 / +	MBON11 > G-Flamp1 & MBON11 > Dop1R1^{RNAi}
Fig. 8k-m	+; 20 x UAS-G-Flamp1 @attP40 / +; R52H01-AD @VK00027, R52B07-DBD @attP2 / Dop1R2^{RNAi} @attP2	MBON11 > G-Flamp1 & MBON11 > Dop1R2^{RNAi}
Supplementary Fig. 1		
Supplementary Fig. 1b	Canton-S	WT
Supplementary Fig. 1c	Canton-S	WT
Supplementary Fig. 1d	Canton-S	WT
Supplementary Fig. 1e	Canton-S	WT
Supplementary Fig. 2		
Supplementary Fig. 2b	20 x UAS-CsChrimson-mVenus @attP18; + / +; R52H01-AD @VK00027, R52B07-DBD @attP2 / +	MBON11 > CsChr
Supplementary Fig. 2b	+; + / +; R52H01-AD @VK00027, R52B07-DBD @attP2 / 20 x UAS-GtACR1-YFP @attP2	MBON11 > GtACR1
Supplementary Fig. 2b	+; UAS-dTrpA1 / +	dTrpA1 / +
	+; UAS-dTrpA1 / +; R52H01-AD @VK00027, R52B07-DBD @attP2 / +	MB085C > dTrpA1
	+; UAS-dTrpA1 / +; R93D10-AD @VK00027, R13F04-DBD @attP2 / +	MB112C > dTrpA1
	+; UAS-dTrpA1 / R52B07-AD @attP40; R52H01-DBD @attP2 / +	MB262B > dTrpA1
	+; tubP-Gal80^{ts} / +; UAS-Kir2.1 / +	G80^{ts} / +; Kir2.1 / +
	+; tubP-Gal80^{ts} / +; R52H01-AD @VK00027, R52B07-DBD @attP2 / UAS-Kir2.1	MB085C > Gal80^{ts}; Kir2.1
	+; tubP-Gal80^{ts} / +; R93D10-AD @VK00027, R13F04-DBD @attP2 / UAS-Kir2.1	MB112C > Gal80^{ts}; Kir2.1
	+; tubP-Gal80^{ts} / R52B07-AD @attP40; R52H01-DBD @attP2 /	MB262B > Gal80^{ts}; Kir2.1

	UAS-Kir2.1	
Supplementary Fig. 2c-e	20 x UAS-CsChrimson-mVenus @attP18; + / +; R52H01-AD @VK00027, R52B07-DBD @attP2 / +	MB085C > CsChr
	20 x UAS-CsChrimson-mVenus @attP18; + / +; R93D10-AD @VK00027, R13F04-DBD @attP2 / +	MB112C > CsChr
	20 x UAS-CsChrimson-mVenus @attP18; R52B07-AD @attP40 / +; R52H01-DBD @attP2 / +	MB262B > CsChr
Supplementary Fig. 2f-h	20 x UAS-CsChrimson-mVenus @attP18; + / +; R52H01-AD @VK00027, R52B07-DBD @attP2 / +	MBON11 > CsChr
Supplementary Fig. 2i	20 x UAS-CsChrimson-mVenus @attP18; + / +; Tk^{FruM}-GAL4 / +	Tk^{FruM} > CsChr
Supplementary Fig. 2j	+; + / +; Tk^{FruM}-GAL4 / +	Tk^{FruM} / +
	+; + / +; Tk^{FruM}-GAL4 / UAS-Kir2.1-eGFP @attP2	Tk^{FruM} > Kir2.1
Supplementary Fig. 2k	20 x UAS-CsChrimson-mVenus @attP18; + / +; R52H01-AD @VK00027, R52B07-DBD @attP2 / +	MBON11 > CsChr
	20 x UAS-CsChrimson-mVenus @attP18; + / +; Tk^{FruM}-GAL4 / +	Tk^{FruM} > CsChr
Supplementary Fig. 2l-m	20 x UAS-CsChrimson-mVenus @attP18; R15A01-AD @attP40 / +; R71G01-DBD @attP2 / +	P1[a] > CsChr
Supplementary Fig. 2n-o	20 x UAS-CsChrimson-mVenus @attP18; + / +; R52H01-AD @VK00027, R52B07-DBD @attP2 / +	MBON11 > CsChr
Supplementary Fig. 2p	Canton-S	WT
Supplementary Fig. 3		
Supplementary Fig. 3d	20 x UAS-CsChrimson-mVenus @attP18; Trh-GAL4 / +; + / +	Trh > CsChr
Supplementary Fig. 3e	13 x LexAop2-CsChrimson-tdtomato @attP18; Trh-LexA::p65 @attP40 / +; 20 x UAS-GCaMP6f @VK00005 / R52H01-GAL4 @attP2	Trh > CsChr & MBON11 > GCaMP6f
Supplementary Fig. 3f	20 x UAS-CsChrimson-mVenus @attP18; VT064246-AD @attP40 /	DPM > CsChr

	+; R13F04-DBD @attP2 / +	
Supplementary Fig. 3g	+; VT064246-AD @attP40 / +; R13F04-DBD @attP2 / 20 x UAS-jGCaMP7f @VK00005	DPM > jGCaMP7f
Supplementary Fig. 3h	20 x UAS-CsChrimson-mVenus @attP18; Tdc2-GAL4 / +; + / +	Tdc2 > CsChr
Supplementary Fig. 3i	+; R12G04-LexA @attP40 / Tdc2-GAL4; 20 x UAS-CsChrimson.mCherry @su(Hw)attP1, 13 x LexAop2-IVS-Syn21-jGCaMP7s-p10 @VK00005 / +	Tdc2 > CsChr & MBON11 > jGCaMP7s
Supplementary Fig. 3i	+; R12G04-LexA @attP40 / +; 20 x UAS-CsChrimson.mCherry @su(Hw)attP1, 13 x LexAop2-IVS-Syn21-jGCaMP7s-p10 @VK00005 / +	empty > CsChr & MBON11 > jGCaMP7s
Supplementary Fig. 3j	13 x LexAop2-CsChrimson-mVenus @attP18; R24E06-AD @attP40 / +; Tdc2-DBD @attP2 / +	MB022B > CsChr
	13 x LexAop2-CsChrimson-mVenus @attP18; R24E06-AD @attP40 / +; R95A10-DBD @attP2 / +	MB021B > CsChr
Supplementary Fig. 3k	+; Tdc2-GAL4 / +; 20 x UAS-jGCaMP7f @VK00005 / +	Tdc2 > jGCaMP7f
Supplementary Fig. 4		
	20 x UAS-CsChrimson-mVenus @attP18; + / +; R52H01-AD @VK00027, R52B07-DBD @attP2 / +	MBON11 > CsChr
Supplementary Fig. 4a	20 x UAS-CsChrimson-mVenus @attP18; + / +; Tk^{FruM}-GAL4 / +	Tk^{FruM} > CsChr
	13 x LexAop2-CsChrimson-mVenus @attP18; R52H01-LexA::p65 @attP40 / +; Tk^{FruM}-GAL4 @attP2 / +	MBON11 > CsChr & Tk^{FruM} > empty
	w-; R52H01-LexA::p65 @attP40 / +; Tk^{FruM}-GAL4 / 20 x UAS-GtACR1-YFP @attP2	MBON11 > empty & Tk^{FruM} > GtACR1
Supplementary Fig. 4b	13 x LexAop2-CsChrimson-mVenus @attP18; R52H01-LexA::p65 @attP40 / +; Tk^{FruM}-GAL4 @attP2 / 20 x UAS-GtACR1-YFP @attP2	MBON11 > CsChr & Tk^{FruM} > GtACR1
Supplementary Fig. 4c	13 x LexAop2-CsChrimson-	MBON11 > CsChr &

	mVenus @attP18; R52H01-LexA::p65 @attP40 / +; Tk^{FruM}-GAL4 @attP2 / +	Tk^{FruM} > empty
	w-; R52H01-LexA::p65 @attP40 / +; Tk^{FruM}-GAL4 / UAS-Kir2.1-eGFP @attP2	MBON11 > empty & Tk^{FruM} > Kir2.1
	13 x LexAop2-CsChrimson-mVenus @attP18; R52H01-LexA::p65 @attP40 / +; Tk^{FruM}-GAL4 @attP2 / UAS-Kir2.1-eGFP @attP2	MBON11 > CsChr & Tk^{FruM} > Kir2.1
Supplementary Fig. 4d-e	13 x LexAop2-CsChrimson-tdtomato @attP18; R52H01-LexA::p65 @attP40 / +; 20 x UAS-GCaMP6f @VK00005 / Tk^{FruM}-GAL4	MBON11 > CsChr & Tk^{FruM} > GCaMP6f
Supplementary Fig. 4d-e	13 x LexAop2-CsChrimson-tdtomato @attP18; + / +; 20 x UAS-GCaMP6f @VK00005 / Tk^{FruM}-GAL4	empty > CsChr & Tk^{FruM} > GCaMP6f
Supplementary Fig. 5		
Supplementary Fig. 5a	+; + / +; R52H01-AD @VK00027, R52B07-DBD @attP2 / 20 x UAS-jGCaMP7f @VK00005	MBON11 > jGCaMP7f
Supplementary Fig. 5b, d, e	13 x LexAop2-jGCaMP7b @su(Hw)attP8; R14E06-LexA @attP40 / +; R52H01-AD @VK00027, R52B07-DBD @attP2 / 20 x UAS-jRGECO1a @VK00005	PPL101 > jGCaMP7b & MBON11 > jRGECO1a
Supplementary Fig. 5c	13 x LexAop2-jGCaMP7b @su(Hw)attP8; R12G04-LexA @attP40 / +; ple-AD @VK00027, R22B12-DBD @attP2 / 20 x UAS-jRGECO1a @VK00005	MBON11 > jGCaMP7b & PPL101 > jRGECO1a
Supplementary Fig. 5f	+; R12G04-LexA @attP40 / R52H03-AD @attP40; 20 x UAS-CsChrimson.mCherry @su(Hw)attP1, 13 x LexAop2-IVS-Syn21-jGCaMP7s-p10 @VK00005 / R14E06-DBD @attP2	PPL101 > CsChr & MBON11 > jGCaMP7s
Supplementary Fig. 5g-h	+; R12G04-LexA @attP40 / R52H03-AD @attP40; 20 x UAS-CsChrimson.mCherry @su(Hw)attP1, 13 x LexAop2-IVS-Syn21-jGCaMP7s-p10 @VK00005 / R14E06-DBD @attP2	PPL101 > CsChr & MBON11 > jGCaMP7s
Supplementary Fig. 5g-h	+; R12G04-LexA @attP40 / +; 20	empty > CsChr &

	x UAS-CsChrimson.mCherry @su(Hw)attP1, 13 x LexAop2-IVS-Syn21-jGCaMP7s-p10 @VK00005	MBON11 > jGCaMP7s
Supplementary Fig. 6		
Supplementary Fig. 6a-d	+; + / +; R52H01-AD @VK00027, R52B07-DBD @attP2 / 20 x UAS-jGCaMP7f @VK00005	MBON11 > jGCaMP7f
Supplementary Fig. 6e-f	20 x UAS-CsChrimson-mVenus @attP18; + / +; R52H01-AD @VK00027, R52B07-DBD @attP2 / +	MBON11 > CsChr
Supplementary Fig. 6g	20 x UAS-CsChrimson-mVenus @attP18; + / +; + / +	CsChr / +
Supplementary Fig. 6j-l	20 x UAS-CsChrimson-mVenus @attP18; + / +; R52H01-AD @VK00027, R52B07-DBD @attP2 / +	MBON11 > CsChr
Fig. 6m	20 x UAS-CsChrimson-mVenus @attP18; + / +; R52H01-AD @VK00027, R52B07-DBD @attP2 / +	MB085C > CsChr
Fig. 6n	20 x UAS-CsChrimson-mVenus @attP18; R52B07-AD @attP40 / +; R52H01-DBD @attP2 / +	MB262B > CsChr
Supplementary Fig. 7		
Supplementary Fig. 7a-k	10 x UAS-mCD8::GFP@su(Hw)attP8; + / +; R52H01-AD @VK00027, R52B07-DBD @attP2 / +	MBON11 > mCD8::GFP
Supplementary Fig. 8		
Supplementary Fig. 8a-b	+; + / +; ple-AD @VK00027, R22B12-DBD @attP2 / UAS-gDA3m @VK00005	PPL101 > gDA3m
Supplementary Fig. 8c-j	10 x UAS-mCD8::GFP @su(Hw)attP8; + / +; R52H01-AD @VK00027, R52B07-DBD @attP2 / +	MBON11 > mCD8::GFP
Supplementary Fig. 9		
Supplementary Fig. 9a	+; UAS-gDA3h @attP40 / +; ple-AD @VK00027, R22B12-DBD @attP2 / +	PPL101 > gDA3h
Supplementary Fig. 9a	+; UAS-gDA3h @attP40 / +; ple-AD @VK00027, R22B12-DBD @attP2 / 20 x UAS-GtACR1-YFP	PPL101 > gDA3h & PPL101 > GtACR1

	@attP2	
Supplementary Fig. 9a	+; UAS-gDA3h @attP40 / +; ple-AD @VK00027, R22B12-DBD @attP2 / 20 x UAS-CsChrimson.mCherry @su(Hw)attP1	PPL101 > gDA3h & PPL101 > CsChr
Supplementary Fig. 9b	+; + / +; R52H01-AD @VK00027, R52B07-DBD @attP2 / +	MB085C / +
	+; Dop1R1^{RNAi} / +; + / +	Dop1R1^{RNAi} / +
	+; + / +; Dop1R2^{RNAi-1} / +	Dop1R2^{RNAi-1} / +
	+; + / +; Dop1R2^{RNAi-2} / +	Dop1R2^{RNAi-2} / +
	+; Dop1R1^{RNAi} / +; R52H01-AD @VK00027, R52B07-DBD @attP2 / +	MB085C > Dop1R1^{RNAi}
	+; + / +; R52H01-AD @VK00027, R52B07-DBD @attP2 / Dop1R2^{RNAi-1}	MB085C > Dop1R2^{RNAi-1}
	+; + / +; R52H01-AD @VK00027, R52B07-DBD @attP2 / Dop1R2^{RNAi-2}	MB085C > Dop1R2^{RNAi-2}
	+; + / +; R52H01-AD @VK00027, R52B07-DBD @attP2 @attP2 / Dop2R^{RNAi}	MB085C > Dop2R^{RNAi}
	+; + / +; R52H01-AD @VK00027, R52B07-DBD @attP2 @attP2 / DopEcR^{RNAi}	MB085C > DopEcR^{RNAi}
Supplementary Fig. 9c	+; + / +; R93D10-AD @VK00027, R13F04-DBD @attP2 / +	MB112C / +
	+; Dop1R1^{RNAi} / +; R93D10-AD @VK00027, R13F04-DBD @attP2 / +	MB112C > Dop1R1^{RNAi}
	+; + / +; R93D10-AD @VK00027, R13F04-DBD @attP2 / Dop1R2^{RNAi}	MB112C > Dop1R2^{RNAi}
	+; + / +; R93D10-AD @VK00027, R13F04-DBD @attP2 / Dop2R^{RNAi}	MB112C > Dop2R^{RNAi}
	+; + / +; R93D10-AD @VK00027, R13F04-DBD @attP2 / DopEcR^{RNAi}	MB112C > DopEcR^{RNAi}
Supplementary Fig. 10		
Supplementary Fig. 10a-d	+; 20 x UAS-jGCaMP7f @su(Hw)attP5 / +; R52H01-AD @VK00027, R52B07-DBD @attP2 / +	MBON11 > jGCaMP7f
Supplementary Fig. 10e-m	+; 20 x UAS-G-Flamp1 @attP40 / +; R52H01-AD @VK00027, R52B07-DBD @attP2 / +	MBON11 > G-Flamp1

Supplementary Table 2

Statistical analyses in each figure.

Figure	Groups	Sample Size	Statistical method	P-value
Fig. 1				
Fig. 1c	WT (no food) vs. WT (food)	33 pairs vs. 30 pairs	two-sided Mann-Whitney U test	9.15E-12
Fig. 1d	WT (fed) vs. WT (hungry)	45 pairs vs. 37 pairs	two-sided Mann-Whitney U test	1.00E-04
Fig. 1e	WT (sucrose rear yeast test) vs. WT (yeast rear yeast test)	35 pairs vs. 30 pairs	two-sided Mann-Whitney U test	3.92E-07
	WT (sucrose rear sucrose test) vs. WT (yeast rear sucrose test)	19 pairs vs. 19 pairs		1.15E-02
Fig. 1f	WT (s, s + AA, s + pep, s + yeast)	20, 23, 23, 23 pairs	Kruskal-Wallis test	2.02E-04
	WT (s) vs. WT (s + AA)	20 pairs vs. 23 pairs	two-sided Mann-Whitney U test	1.76E-02
	WT (s) vs. WT (s + pep)	20 pairs vs. 23 pairs		6.24E-04
	WT (s) vs. WT (s + yeast)	20 pairs vs. 23 pairs		7.60E-05
	WT (s + AA) vs. WT (s + pep)	23 pairs vs. 23 pairs		0.29
	WT (s + AA) vs. WT (s + yeast)	23 pairs vs. 23 pairs		4.21E-02
	WT (s + pep) vs. WT (s + yeast)	23 pairs vs. 23 pairs		0.26
Fig. 2				
Fig. 2a	MB085C > CsChr vs. MB085C / +	153 pairs vs. 33 pairs	two-sided Mann-Whitney U test	1.51E-17
	MB085C > CsChr vs. CsChr / +	153 pairs vs. 35 pairs		4.06E-19
	MB085C > GtACR1 vs. MB085C / +	32 pairs vs. 21 pairs		3.91E-09
	MB085C > GtACR1 vs. GtACR1 / +	32 pairs vs. 53 pairs		1.82E-13
	MB112C / + vs. MB112C > CsChr	34 pairs vs. 28 pairs		1.60E-04
	CsChr / + vs. MB112C > CsChr	35 pairs vs. 28 pairs		2.95E-08
	MB262B / + vs. MB262B > CsChr	17 pairs vs. 23 pairs		5.06E-06
	CsChr / + vs.	35 pairs vs. 23		1.01E-08

	MB262B > CsChr	pairs		
	GtACR1 / + vs. MB112C > GtACR1	53 pairs vs. 40 pairs		5.77E-16
	MB112C / + vs. MB112C > GtACR1	33 pairs vs. 40 pairs		7.49E-13
	GtACR1 / + vs. MB262B > GtACR1	53 pairs vs. 19 pairs		3.89E-10
	MB262B / + vs. MB262B > GtACR1	19 pairs vs. 19 pairs		4.30E-07
Fig. 2b	MBON11 > CsChr (no food) pre vs. dur	33 pairs	two-sided Wilcoxon matched-pairs signed rank test	2.50E-03
	MBON11 > CsChr (food) pre vs. dur	20 pairs		5.74E-06
	MBON11 > CsChr (no food) dur vs. MBON11 > CsChr (food) dur	33 pairs vs. 20 pairs	two-sided Mann-Whitney U test	1.64E-09
Fig. 2c	MBON11 > CsChr (fed) pre vs. dur	22 pairs	two-sided Wilcoxon matched-pairs signed rank test	4.77E-07
	MBON11 > CsChr (hungry) pre vs. dur	23 pairs		3.30E-05
	MBON11 > CsChr (fed) dur vs. MBON11 > CsChr (hungry) dur	22 pairs vs. 23 pairs	two-sided Mann-Whitney U test	0.97
Fig. 2d	MBON11 > CsChr (sucrose rear yeast test, yeast rear yeast test, sucrose rear sucrose test, yeast rear sucrose test)	21, 26, 23, 18 pairs	Kruskal-Wallis test	0.20
Fig. 2e	MBON11 > Kir2.1 (sucrose rear yeast test)	15 pairs		
	MBON11 > Kir2.1 (yeast rear yeast test)	15 pairs		
	MBON11 > Kir2.1 (sucrose rear sucrose test)	16 pairs		
	MBON11 > Kir2.1 (yeast rear sucrose test)	16 pairs		
Fig. 2f	MBON11 > CsChr (s, s + AA, s + pep, s + yeast) dur	12, 12, 12, 12 pairs	Kruskal-Wallis test	0.56

Fig. 2g	MBON11 > Kir2.1 (s, s + AA, s + pep, s + yeast)	12, 12, 11, 12 pairs	Kruskal-Wallis test	0.92
Fig. 2i	touch apple juice food vs. touch agarose	10 flies vs. 11 flies	two-sided Mann-Whitney U test	3.60E-02
Fig. 2j	Hungry vs. fed	40 flies vs. 18 flies	two-sided Mann-Whitney U test	2.04E-05
Fig. 2k	Sucrose vs. Sucrose + AA	14 flies vs. 21 flies	two-sided Mann-Whitney U test	3.10E-02
Fig. 3				
Fig. 3d	GtACR1 / + vs. MB502B > GtACR1	11 pairs vs. 35 pairs	two-sided Mann-Whitney U test	2.77E-06
	GtACR1 / + vs. MB320C > GtACR1	11 pairs vs. 32 pairs		1.40E-04
	GtACR1 / + vs. MB438B > GtACR1	11 pairs vs. 21 pairs		2.20E-04
	MB502B / + vs. MB502B > GtACR1	11 pairs vs. 35 pairs		2.77E-06
Fig. 3e	PPL101 / + pre vs. dur	14 pairs	two-sided Wilcoxon matched-pairs signed rank test	0.49
	CsChr / + pre vs. dur	10 pairs		0.48
	PPL101 > CsChr pre vs. dur	10 pairs		8.00E-03
	PPL101 / + dur vs. PPL101 > CsChr dur	14 pairs vs. 10 pairs	two-sided Mann-Whitney U test	3.10E-04
	CsChr / + dur vs. PPL101 > CsChr dur	10 pairs vs. 10 pairs		5.70E-04
Fig. 3f	PPL101 / + vs. PPL101 > Caspase-3	24 pairs vs. 20 pairs	two-sided Mann-Whitney U test	8.90E-07
	PPL101 / + vs. PPL101 > Reaper & Grim	24 pairs vs. 33 pairs		9.85E-06
	Caspase-3 / + vs. PPL101 > Caspase-3	14 pairs vs. 20 pairs		2.48E-05
	Reaper & Grim / + vs. PPL101 > Reaper & Grim	19 pairs vs. 33 pairs		1.04E-05
Fig. 3h	Fed vs. Hungry	10 flies vs. 8 flies	two-sided Mann-Whitney U test	1.20E-02

Fig. 3i	Sucrose vs. Sucrose + AA	17 flies vs. 17 flies	two-sided Mann-Whitney U test	2.60E-02
Fig. 4				
Fig. 4b	GtACR1 / +	12 pairs		
	PPL101 / +	11 pairs		
	MBON11 /+	19 pairs		
	PPL101 > GtACR1 pre vs. dur	7 pairs	two-sided Wilcoxon matched-pairs signed rank test	1.60E-02
	MBON11 > GtACR1 pre vs. dur	11 pairs		9.80E-04
	MBON11 >GtACR1 & PPL101> GtACR1 pre vs. dur	18 pairs		2.10E-04
	PPL101 > GtACR1 dur vs. MBON11> GtACR1 dur	7 pairs vs. 11 pairs	two-sided Mann-Whitney U test	5.70E-04
	PPL101 > GtACR1 dur vs. MBON11 > GtACR1 & PPL101 > GtACR1 dur	7 pairs vs. 18 pairs		1.50E-04
	MBON11 > GtACR1 dur vs. MBON11 > GtACR1 & PPL101 > GtACR1 dur	11 pairs vs. 18 pairs		0.10
Fig. 4d	CsChr / +	11 pairs		
	Kir2.1 / +	11 pairs		
	PPL101; MBON11 / +	12 pairs		
	CsChr; Kir2.1 / +	24 pairs		
	PPL101 > empty & MBON11 > CsChr pre vs. dur	14 pairs	two-sided Wilcoxon matched-pairs signed rank test	1.20E-04
	PPL101 > Kir2.1 & MBON11 > empty pre vs. dur	12 pairs		0.07
	PPL101 > Kir2.1 & MBON11 > CsChr pre vs. dur	25 pairs		3.40E-03
	PPL101 > empty & MBON11 > CsChr dur vs. PPL101 > Kir2.1 & MBON11 > CsChr dur	14 pairs vs. 25 pairs	two-sided Mann-Whitney U test	0.65
	PPL101 > Kir2.1 & MBON11 > empty dur vs. PPL101 > Kir2.1 & MBON11 > CsChr dur	12 pairs vs. 25 pairs		2.20E-04
Fig. 4e	PPL101 > empty &	14 pairs		

	MBON11 > CsChr			
	PPL101 > Kir2.1 & MBON11 > CsChr	25 pairs		
Fig. 4g	GtACR1 / +	24 pairs		
	CsChr / +	22 pairs		
	CsChr; GtACR1 / +	19 pairs		
	MBON11; Tk^{FruM} / +	19 pairs		
	MBON11 > CsChr & Tk^{FruM} > empty R vs. R+G	22 pairs	two-sided Wilcoxon matched-pairs signed rank test	9.87E-05
	MBON11 > empty & Tk^{FruM} > GtACR1 R vs. R+G	24 pairs		1.19E-07
	MBON11 > CsChr & Tk^{FruM} > GtACR1 R vs. R+G	24 pairs		1.19E-07
	MBON11 > CsChr & Tk^{FruM} > empty R+G vs. MBON11 > empty & Tk^{FruM} > GtACR1 R+G	22 pairs vs. 24 pairs	two-sided Mann-Whitney U test	6.86E-09
	MBON11 > CsChr & Tk^{FruM} > empty R+G vs. MBON11 > CsChr & Tk^{FruM} > GtACR1 R+G	22 pairs vs. 24 pairs		6.78E-09
	MBON11 > empty & Tk^{FruM} > GtACR1 R+G vs. MBON11 > CsChr & Tk^{FruM} > GtACR1 R+G	24 pairs vs. 24 pairs		0.52
Fig. 5				
Fig. 5c-d	Fed	12flies		
	Hungry	10 flies		
Fig. 5e	Fed	12 flies		
	Hungry	17 flies		
Fig. 5f	MBON11 (Fed, Hungry)	18, 40 flies (replot Fig. 2j)		
	PPL101 (Fed, Hungry)	10, 8 flies (replot Fig. 3h)		
Fig. 5g	MBON11 (Sucrose, Sucrose + AA)	14, 21 flies (replot Fig. 2k)		
	PPL101 (Sucrose, Sucrose + AA)	17, 17 flies (replot Fig. 3i)		

Fig. 6				
Fig. 6a	WT vs. MBON11 > CsChr	14,17,23 pairs vs. 20, 19, 22 pairs	two-sided Mann-Whitney U test	3.75E-08
Fig. 6c	MBON11 > Kir2.1 (0 h, 7 h, 14 h)	9, 16, 11 pairs		
	WT vs. MBON11 > CsChr	34, 23, 35 pairs vs. 22, 23, 17 pairs (replot Fig. 2c)	two-sided Mann-Whitney U test	8.49E-09
	WT vs. MBON11 > Kir2.1	34, 23, 35 pairs vs. 9, 16, 11 pairs	two-sided Mann-Whitney U test	6.16E-06
	MBON11 > CsChr vs. MBON11 > Kir2.1	22, 23, 17 pairs vs. 9, 16, 11 pairs	two-sided Mann-Whitney U test	6.45E-11
Fig. 6g AUC	0-0.5 h, 3-5 h, 6-8 h, 8-10 h, 10-12 h, 12-14 h, 14-16 h	18, 8, 10, 9, 10, 11, 10 flies	Kruskal-Wallis test	2.20E-03
	0-0.5 h vs. 10-12 h	18 flies vs. 10 flies	Dunn's multiple comparisons test	2.20E-02
	0-0.5 h vs. 12-14 h	18 flies vs. 11 flies		1.70E-02
	0-0.5 h vs. 14-16 h	18 flies vs. 10 flies		3.70E-02
Fig. 6i	0 mM, 50 mM, 100 mM, 200 mM, Apple juice food	20, 19, 22, 19, 48 pairs (replot Fig. 6a)		
Fig. 6j	0.5 mW 50Hz 10 ms	153 pairs (pooling Fig. 6i 48 pairs and Supplementary Fig. 2c 56 pairs)	Pearson Correlation Coefficient	6.60E-37
	1 mW 50Hz 10 ms	108 pairs (pooling Fig. 2b 20 pairs)	Pearson Correlation Coefficient	2.50E-23
	2 mW 50Hz 10 ms	56 pairs	Pearson Correlation Coefficient	4.39E-07
Fig. 6k	0 h (refeeding & starvation)	63 pairs (pooling Fig. 1d 45 pairs)	Pearson Correlation Coefficient	1.30E-05

	7 h (refeeding & starvation)	44 pairs	Pearson Correlation Coefficient	1.80E-03
	14 h (refeeding & starvation)	63 pairs (pooling Fig. 1d 37 pairs)	Pearson Correlation Coefficient	6.84E-03
Fig. 6o	Hungry vs. Fed	8 flies vs. 4 flies	Two-way ANOVA	5.00E-03
Fig. 7				
Fig. 7c	Fed vs. hungry	9 flies vs. 12 flies	two-sided Mann-Whitney U test	3.40E-02
Fig. 7e	Control vs. TH^{RNAi}	43 trials vs. 63 trials	two-sided Mann-Whitney U test	1.05E-10
Fig. 7g	Fed vs. Hungry	88 trials vs. 103 trials	two-sided Mann-Whitney U test	8.51E-05
Fig. 7i	Saline vs. DA	10 flies vs. 10 flies	One-way ANOVA	3.97E-03
Fig. 7l	Pre DA vs. Post DA	5 flies	Two-way ANOVA	1.50E-04
Fig. 7m	PPL101 / + vs. PPL101 > TH^{RNAi}	20 pairs vs. 22 pairs	two-sided Mann-Whitney U test	6.52E-05
	TH^{RNAi} / + vs. PPL101 > TH^{RNAi}	13 pairs vs. 22 pairs		1.60E-04
Fig. 7o	MBON11 / + vs. MBON11 > $Dop1R1^{RNAi}$	43 pairs vs. 30 pairs	two-sided Mann-Whitney U test	3.58E-11
	MBON11 / + vs. MBON11 > $Dop1R2^{RNAi}$	43 pairs vs. 57 pairs		4.29E-17
	$Dop1R1^{RNAi}$ / + vs. MBON11 > $Dop1R1^{RNAi}$	23 pairs vs. 30 pairs		1.50E-08
	$Dop1R2^{RNAi}$/ + vs. MBON11 > $Dop1R2^{RNAi}$	16 pairs vs. 57 pairs		2.45E-08
Fig. 8				
Fig. 8c	ACV vs. ACV + DA↑	15 flies vs. 9	two-sided	2.80E-02

		flies	Mann-Whitney U test	
Fig. 8c	ACV vs. ACV + DA↓	15 flies vs. 11 flies	two-sided Mann-Whitney U test	1.80E-02
Fig. 8e	Control vs. $Dop1R1^{RNAi}$	9 flies vs. 12 flies (replot Fig. 8c)	two-sided Mann-Whitney U test	4.90E-02
Fig. 8e	Control vs. $Dop1R2^{RNAi}$	9 flies vs. 14 flies	two-sided Mann-Whitney U test	0.78
Fig. 8g	Control vs. $Dop1R1^{RNAi}$	11 flies vs. 12 flies (replot Fig. 8c)	two-sided Mann-Whitney U test	0.61
Fig. 8g	Control vs. $Dop1R2^{RNAi}$	11 flies vs. 9 flies	two-sided Mann-Whitney U test	1.10E-03
Fig. 8j	Control vs. $Dop1R1^{RNAi}$	15 flies vs. 20 flies	two-sided Mann-Whitney U test	0.83
Fig. 8j	Control vs. $Dop1R2^{RNAi}$	15 flies vs. 26 flies	two-sided Mann-Whitney U test	1.10E-03
Fig. 8m	Control vs. $Dop1R1^{RNAi}$	18 flies vs. 13 flies	two-sided Mann-Whitney U test	6.00E-04
Fig. 8m	Control vs. $Dop1R2^{RNAi}$	18 flies vs. 10 flies	two-sided Mann-Whitney U test	0.10
Supplementary Fig. 1				
Supplementary Fig. 1b	WT (no food) vs. WT (food)	33 pairs vs. 30 pairs	two-sided Mann-Whitney U test	1.11E-11
Supplementary Fig. 1c	WT (fed) vs. WT (hungry)	45 pairs vs. 37 pairs	two-sided Mann-Whitney U test	5.00E-04
Supplementary Fig. 1d				
	WT (fed) vs. WT (hungry)	45 pairs vs. 37 pairs (replot Fig. 1d)	two-sided Mann-Whitney U test	1.00E-04
	WT (fed) vs. WT	45 pairs vs.63		0.36

	(refeed)	pairs (replot Fig. 6k)		
	WT (hungry) vs. WT (refeed)	37 pairs vs. 63 pairs		9.70E-07
Supplementary Fig. 1e	WT (0x) vs. WT (0.5 x)	12 pairs vs. 11pairs	two-sided Mann-Whitney U test	0.31
	WT (0 x) vs. WT (1 x)	12 pairs vs. 12 pairs		1.94E-02
	WT (0 x) vs. WT (2 x)	12 pairs vs. 12 pairs		0.05
Supplementary Fig. 2				
Supplementary Fig. 2b	dTrpA1 / + (29°C) vs. MB085C > dTrpA1(29°C)	34 pairs vs. 56 pairs	two-sided Mann-Whitney U test	3.56E-12
	dTrpA1 / + (29°C) vs. MB112C > TrpA1 (29°C)	34 pairs vs. 33 pairs		4.36E-11
	dTrpA1 / + (29°C) vs. MB262B > TrpA1 (29°C)	34 pairs vs. 22 pairs		2.70E-02
	GAL80; Kir2.1 /+ (25°C) vs. MB085C > GAL80; Kir2.1 (25°C)	31 pairs vs. 32 pairs		3.50E-04
	GAL80; Kir2.1 /+ (25°C) vs. MB112C > GAL80; Kir2.1 (25°C)	31 pairs vs. 55 pairs		3.64E-07
	GAL80; Kir2.1 /+ (25°C) vs. MB262B > GAL80; Kir2.1 (25°C)	31 pairs vs. 23 pairs		3.56E-07
Supplementary Fig. 2c				
	MB085C > CsChr pre vs. dur	56 pairs	two-sided Wilcoxon matched-pairs signed rank test	7.55E-11
	MB112C > CsChr pre vs. dur	28 pairs		7.45E-09
	MB262B > CsChr pre vs. dur	23 pairs		2.38E-07
Supplementary Fig. 2d	MB085C > CsChr pre vs. dur	56 pairs	two-sided Wilcoxon matched-pairs signed rank test	1.08E-08
	MB112C > CsChr pre vs. dur	28 pairs		6.35E-02
	MB262B > CsChr pre vs. dur	23 pairs		1.53E-04
Supplementary Fig. 2e	MB085C > CsChr pre vs. dur	12 pairs	two-sided Wilcoxon matched-pairs signed rank	0.10
	MB112C > CsChr pre vs. dur	12 pairs		0.064

	MB262B > CsChr pre vs. dur	12 pairs	test	0.20
Supplementary Fig. 2f	MBON11 > CsChr (no food) pre vs. dur	33 pairs (replot Fig. 2b)	two-sided Wilcoxon matched-pairs signed rank test	2.50E-03
	MBON11 > CsChr (male-male food) pre vs. dur	20 pairs (replot Fig. 2b)		5.74E-06
	MBON11 > CsChr (tethered female) pre vs. dur	18 pairs		1.91E-06
	MBON11 > CsChr (male-female food) pre vs. dur	12 pairs		1
	MBON11 > CsChr (no food) dur vs. MBON11>CsChr (male-male food) dur	33 pairs vs. 20 pairs	two-sided Mann-Whitney U test	1.64E-09
Supplementary Fig. 2g	MBON11 > CsChr (no food) pre vs. dur	33 pairs	two-sided Wilcoxon matched-pairs signed rank test	2.34E-05
	MBON11 > CsChr (male-male food) pre vs. dur	20 pairs		9.54E-06
	MBON11 > CsChr (tethered female) pre vs. dur	18 pairs		1
	MBON11 > CsChr (male-female food) pre vs. dur	12 pairs		1
	MBON11 > CsChr (no food) dur vs. MBON11>CsChr (male-male food) dur	33 pairs vs. 20 pairs	two-sided Mann-Whitney U test	4.08E-07
Supplementary Fig. 2h				
	MBON11 > CsChr (no food) pre vs. dur	33 pairs	two-sided Wilcoxon matched-pairs signed rank test	3.14E-05
	MBON11 > CsChr (male-male food) pre vs. dur	20 pairs		1.70E-04
	MBON11 > CsChr (tethered female) pre vs. dur	18 pairs		0.0665
	MBON11 > CsChr (male-female food) pre vs. dur	12 pairs (replot Supplementary Fig. 2e)		0.09
Supplementary Fig. 2i	Tk^{FruM} > CsChr pre vs. dur	114 pairs	two-sided Wilcoxon matched-pairs	5.60E-16

			signed rank test	
Supplementary Fig. 2j	Tk^{FruM} / + vs. Tk^{FruM} > Kir2.1	24 pairs vs. 40 pairs	two-sided Mann-Whitney U test	1.05E-09
Supplementary Fig. 2k	MBON11 > CsChr vs. Tk^{FruM} > CsChr	12 pairs vs. 12 pairs	two-sided Mann-Whitney U test	3.37E-05
Supplementary Fig. 2l	$P1^{a}$ > CsChr pre vs. dur	23 pairs	two-sided Wilcoxon matched-pairs signed rank test	0.89
Supplementary Fig. 2m	$P1^{a}$ > CsChr pre vs. dur	23 pairs	two-sided Wilcoxon matched-pairs signed rank test	1.19E-06
Supplementary Fig. 2n	MBON11 > CsChr (sucrose rear yeast test, yeast rear yeast test, sucrose rear sucrose test, yeast rear sucrose test)	21,26,23,18 pairs (replot Fig. 2d)		
Supplementary Fig. 2o	MBON11 > CsChr (s, s + AA, s + peptone, s + yeast)	12, 12, 12, 12 pairs (replot Fig. 2f)		
Supplementary Fig. 2p	Sucrose + AA, Sucrose, Hungry (Lunge frequency)	23 pairs, 20 pairs, 37 pairs (replot Fig. 1d, Fig. 1f)		
	Sucrose + AA, Sucrose, Hungry (MBON11 response)	21, 14, 40 pairs (replot Fig. 2j, Fig. 2k)		
Supplementary Fig. 3				
Supplementary Fig. 3d	Trh > CsChr pre vs. dur	93 pairs	two-sided Wilcoxon matched-pairs signed rank test	2.48E-14
Supplement	DPM > CsChr pre vs.	12 pairs	two-sided	0.27

ary Fig. 3f	dur		Wilcoxon matched-pairs signed rank test	
Supplementary Fig. 3g	Sucrose vs. Sucrose + AA	10 flies vs. 9 flies	two-sided Mann-Whitney U test	0.84
Supplementary Fig. 3h	Tdc2 > CsChr pre vs. dur	12 pairs	two-sided Wilcoxon matched-pairs signed rank test	9.80E-04
Supplementary Fig. 3i	Control vs. Photostim	8 flies vs. 6 flies	two-sided Mann-Whitney U test	2.40E-03
Supplementary Fig. 3j	MB021B > CsChr pre vs. dur	12 pairs	two-sided Wilcoxon matched-pairs signed rank test	0.34
	MB022B > CsChr pre vs. dur	12 pairs		4.90E-03
Supplementary Fig. 3k	Sucrose vs. Sucrose + AA	8 flies vs. 7 flies	two-sided Mann-Whitney U test	0.87
Supplementary Fig. 4				
Supplementary Fig. 4b	MBON11 > CsChr & Tk^{FruM} > empty	22 pairs		
	MBON11 > empty & Tk^{FruM} > GtACR1	24 pairs		
	MBON11 > CsChr & Tk^{FruM} > GtACR1	24 pairs		
Supplementary Fig. 4c	MBON11 > CsChr & Tk^{FruM} > empty pre vs. dur	20 pairs	two-sided Wilcoxon matched-pairs signed rank test	9.54E-06
	MBON11>empty & Tk^{FruM} > Kir2.1 pre vs. dur	27 pairs		0.83
	MBON11 > CsChr & Tk^{FruM} > Kir2.1 pre vs. dur	25 pairs		2.99E-05
	MBON11 > CsChr & Tk^{FruM} > empty dur vs. MBON11 > empty & Tk^{FruM} > Kir2.1 dur	20 pairs vs.27 pairs	two-sided Mann-Whitney U test	1.48E-06
	MBON11 > CsChr &	20 pairs vs.25		2.11E-06

	Tk^{FruM} > empty dur vs. MBON11 > CsChr & Tk^{FruM} > Kir2.1 dur	pairs		
	MBON11 > empty & Tk^{FruM} > Kir2.1 dur vs. MBON11 > CsChr & Tk^{FruM} > Kir2.1 dur	27 pairs vs. 25 pairs		0.58
Supplementary Fig. 4e	MBON11 to Tk^{FruM} pre vs. post	11 flies	two-sided Wilcoxon matched-pairs signed rank test	6.80E-03
	Empty to Tk^{FruM} pre vs. post	10 flies	two-sided Wilcoxon matched-pairs signed rank test	0.56
Supplementary Fig. 5				
Supplementary Fig. 5c	Fed vs. Hungry	143 trials vs. 114 trials	two-sided Mann-Whitney U test	4.41E-08
Supplementary Fig. 5d	Fed vs. Hungry	133 trials vs. 187 trials	two-sided Mann-Whitney U test	3.10E-02
Supplementary Fig. 5g	low control, low power, high control, high power	118 trials in 11 flies, 64 trials in 8 flies, 111 trials in 10 flies, 97 trials in 9 flies	Kruskal-Wallis test	5.46E-08
	low control vs. low power	118 trials in 11 flies vs. 64 trials in 8 flies	Dunn's multiple comparisons test	1.90E-03
	high control vs. high power	111 trials in 10 flies vs. 97 trials in 9 flies		5.02E-07
	low control vs. high control	118 trials in 11 flies vs. 111 trials in 10 flies		>0.99
	low power vs. high power	64 trials in 8 flies vs. 97 trials in 9 flies		3.00E-04
Supplementary Fig. 6				
Supplementary Fig. 6c	0-0.5 h, 3-8 h, 9-12 h, 12-16 h	18, 18, 19, 21 flies	Kruskal-Wallis test	4.40E-03

	0-0.5 vs. 9-12	18 flies vs. 19 flies	Dunn's multiple comparisons test	5.70E-03
	0-0.5 vs. 12-16	18 flies vs. 21 flies		2.70E-02
Supplementary Fig. 6e-f	0.5 mW / cm^2, 1 mW / cm^2, 2 mW / cm^2	153, 108, 56 pairs	Kruskal-Wallis test	1.30E-04
	0.5 mW / cm^2 vs. 1 mW / cm^2	153 pairs vs. 108 pairs	two-sided Mann-Whitney U test	1.65E-02
	0.5 mW / cm^2 vs. 2 mW / cm^2	153 pairs vs. 56 pairs		5.54E-05
	1 mW / cm^2 vs. 2 mW / cm^2	108 pairs vs. 56 pairs		3.10E-02
Supplementary Fig. 6g	CsChr / +	35 pairs		
Supplementary Fig. 6j	MBON11 > CsChr (0 mM) pre vs. dur	20 pairs (replot Fig. 6i)	two-sided Wilcoxon matched-pairs signed rank test	6.40E-03
	MBON11 > CsChr (50 mM) pre vs. dur	19 pairs (replot Fig. 6i)		7.25E-05
	MBON11 > CsChr (100 mM) pre vs. dur	22 pairs (replot Fig. 6i)		6.68E-06
	MBON11 > CsChr (200 mM) pre vs. dur	19 pairs (replot Fig. 6i)		7.25E-05
	MBON11 > CsChr (Apple juice food) pre vs. dur	48 pairs (replot Fig. 6i)		7.11E-15
Supplementary Fig. 6k	MBON11 > CsChr (0 mM, 50 mM, 100 mM, 200 mM)	14, 19, 20, 19, 48 pairs	Kruskal-Wallis test	8.72E-15
Supplementary Fig. 6l	MBON11 > CsChr (0 mM, 50 mM, 100 mM, 200 mM)	14, 19, 20, 19, 48 pairs	Kruskal-Wallis test	0.13
Supplementary Fig. 6m	0.5 mW 50 Hz 10 ms pre vs. dur	12 pairs	two-sided Wilcoxon matched-pairs signed rank test	0.33
	1 mW 50 Hz 10 ms pre vs. dur	33 pairs (replot Fig. 2b)		5.61E-06
	1 mW continuous pre vs. dur	35 pairs		9.05E-06
Supplementary Fig. 6n	1 mW 50 Hz 10 ms pre vs. dur	12 pairs	two-sided Wilcoxon matched-pairs signed rank test	0.05
	1 mW continuous pre vs. dur	9 pairs		2.04E-02
Supplementary Fig. 7				

Supplementary Fig. 7d	Hungry vs. Fed	3 flies vs. 3 flies	two-sided Mann-Whitney U test	<0.001
Supplementary Fig. 7j	Hungry vs. Fed	8 flies vs. 4 flies	Two-way ANOVA	1.60E-03
Supplementary Fig. 7k	Hungry vs. Fed	8 flies vs. 4 flies	Two-way ANOVA	5.00E-03
Supplementary Fig. 8				
Supplementary Fig. 8b	Fed vs. Hungry	156 trials vs. 137 trials	two-sided Mann-Whitney U test	3.20E-03
Supplementary Fig. 8f	Pre puff vs. Post puff	11 flies	two-sided Wilcoxon Signed Rank Test	3.90E-03
Supplementary Fig. 8i	Pre DA vs. Post DA	5 flies	Two-way ANOVA	1.2E-04
Supplementary Fig. 8j	Pre DA vs. Post DA	5 flies	Two-way ANOVA	9.62E-07
Supplementary Fig. 9				
Supplementary Fig. 9a	CsChr pre vs. post	4 flies	two-sided Paired t test	2.20E-02
Supplementary Fig. 9a	GtACR1 pre vs. post	9 flies	two-sided Paired t test	4.90E-03
Supplementary Fig. 9a	No opsin pre vs. post	4 flies	two-sided Paired t test	0.74
Supplementary Fig. 9b	MB085C / + vs. MB085C > Dop1R1^{RNAi}	43 pairs vs. 30 pairs (replot Fig. 7o)	two-sided Mann-Whitney U test	3.58E-11
	MB085C / + vs. MB085C > Dop1R2^{RNAi-1}	43 pairs vs. 57 pairs (replot Fig. 7o)		4.29E-17
	MB085C / + vs. MB085C > Dop2R^{RNAi}	43 pairs vs. 21 pairs		5.30E-03
	MB085C / + vs. MB085C > DopEcR^{RNAi}	43 pairs vs. 20 pairs		7.35E-05
	Dop1R1^{RNAi} / + vs. MB085C >	23 pairs vs. 30 pairs		1.50E-08

	Dop1R1^{RNAi}	(replot Fig. 7o)		
	Dop1R2^{RNAi-1} / + vs. MB085C > Dop1R2^{RNAi-1}	16 pairs vs. 57 pairs (replot Fig. 7o)		2.45E-08
	MB085C / + vs. MB085C > Dop1R2^{RNAi-2}	43 pairs vs. 21 pairs		1.02E-09
	Dop1R2^{RNAi-2} / + vs. MB085C > Dop1R2^{RNAi-2}	24 pairs vs. 21 pairs		3.82E-05
Supplementary Fig. 9c	MB112C / + vs. MB112C > Dop1R1^{RNAi}	40 pairs vs. 59 pairs	two-sided Mann-Whitney U test	3.62E-09
	MB112C / + vs. MB112C > Dop1R2^{RNAi}	40 pairs vs. 54 pairs		1.17E-08
	MB112C / + vs. MB112C > Dop2R^{RNAi}	40 pairs vs. 22 pairs		0.46
	MB112C / + vs. MB112C > DopEcR^{RNAi}	40 pairs vs. 15 pairs		2.10E-02
Supplementary Fig. 10				
Supplementary Fig. 10b	Control vs. YM-254890	9 flies vs. 6 flies (replot Fig. 8b)	two-sided Mann-Whitney U test	0.69
Supplementary Fig. 10d	Control vs. YM-254890	11 flies vs. 9 flies (replot Fig. 8b)	two-sided Mann-Whitney U test	1.60E-02
Supplementary Fig. 10g	ACV vs. control	16 flies vs. 8 flies	two-sided Mann-Whitney U test	1.10E-03
Supplementary Fig. 10j	Forskolin vs. control	4 flies vs. 8 flies	two-sided Mann-Whitney U test	8.50E-03
Supplementary Fig. 10m	ACV vs. ACV + DA↑	16 flies vs. 12 flies	two-sided Mann-Whitney U test	3.10E-02
Supplementary Fig. 10m	ACV vs. ACV + DA↓	16 flies vs. 10 flies	two-sided Mann-Whitney U test	0.65